UNIVERSITATEA **POLITEHNICA** DIN BUCUREŞTI
Facultatea de Știința și Ingineria Materialelor
Departamentul de Ingineria și Managementul Obținerii Materialelor Metalice

THESIS

COMPOZITE IN-SITU CU MATRICE DE ALUMINIU ȘI PARTICULE DE ZrB_2

IN-SITU COMPOSITES WITH ALUMINUM MATRIX AND ZrB_2 PARTICLES

Author
Ing. Lucian ROȘU

PhD supervisor
Prof. dr. ing. Petru MOLDOVAN

Bucharest, 2021

Contents

Keywords

Composites
Metal Matrix Composites (MMC)
Particles
Fibers
In Situ
Processing
Reinforcement
Aluminium metal matrix composites (AMCs)
Zirconium diboride (ZrB_2)
Ceramic Reinforcement
Casting
Aluminium

Introduction

Metal composite materials have found application in many areas of daily life for quite some time. Often it is not realized that the application makes use of composite materials. These materials are produced in situ from the conventional production and processing of metals [1].

Materials like cast iron with graphite or steel with a high carbide content, as well as tungsten carbides, consisting of carbides and metallic binders, also belong to this group of composite materials. For many researchers the term metal matrix composites is often equated with the term light metal matrix composites (MMCs). [1]

Substantial progress in the development of light metal matrix composites has been achieved in recent decades, so that they could be introduced into the most important applications. In traffic engineering, especially in the automotive industry, MMCs have been used commercially in fibre reinforced pistons and aluminium crank cases with strengthened cylinder surfaces as well as particle-strengthened brake disks. [1]

These innovative materials open up unlimited possibilities for modern material science and development; the characteristics of MMCs can be designed into the material, custom-made, dependent on the application. From this potential, metal matrix composites fulfill all the desired conceptions of the designer. This material group becomes interesting for use as constructional and functional materials, if the property profile of conventional materials either does not reach the increased standards of specific demands or is the solution of the problem. However, the technology of MMCs is in competition with other modern material technologies, for example powder metallurgy. The advantages of the composite materials are only realized when there is a reasonable cost – performance relationship in the component production. The use of a composite material is obligatory if a special property profile can only be achieved by application of these materials. [1]

Titanium, aluminium and magnesium alloys are the most popular matrix metals presently in vogue, which are particularly suitable for automobile, defence, structural and aircraft applications [1]. In the last three decades, metal matrix composites (MMCs) have the potential to replace the conventional materials in several fields of applications like transportation, military, marine as well as in various advanced engineering industries [2].

Aluminium matrix composites (AMCs) are being considered as a group of advanced materials for their lightweight, low thermal expansion coefficient, outstanding wear resistance properties and good mechanical properties [3].

Extensively employed fabrication methods for aluminium matrix composites involve stir casting, compo casting, vacuum casting, powder metallurgy, centrifugal casting, insitu casting and squeeze casting [4-5]. Among those available process, in situ method is most economical and is always preferred. In situ formed particles reveal strong interfacial bonding with the matrix. In situ method overcomes the limitations of stir casting process such as improper wetting of reinforcement particles and density dependence of particles and its associated problems like sinking and floating of particles [6]. In situ ceramic particles, such as Al_2O_3, TiB_2, AlN, TiC, B_4C and ZrB_2 have been widely used as reinforcements in aluminium-based composites [7].

The particular attributes of aluminium composites are a combination of high specific stiffness, good fatigue properties, and the potential for relatively low-cost conventional processing. It is also possible to tailor the mechanical and thermal properties of these materials to meet the requirements of a specific application. To do this there are a number of variables which need to be considered, which include the type and level of reinforcement, the choice of matrix alloy, and the composite processing route. All these factors are inter-related and should not be considered in isolation when developing a new material [8].

Aluminium composites have been under development for many years during which time a vast number of different types of reinforcement have been attempted with varying degrees of success [9]. These include continuous fibres, both monofilament and multifilament, short fibres, whiskers and particulates [10]. Many different matrices have been tried over the years and these have a bearing on some of the properties that can be achieved in the composite. Corrosion resistance, strength levels, toughness etc. are all strongly influenced by the matrix alloy [11]. Generally standard engineering alloys are used but in a slightly modified form to accept the selected reinforcement.

The type of reinforcement also influences the method of manufacture, continuous monofilament needs to be handled in a different way to particulate or even short fibre reinforcement. The aluminium composites currently under consideration, by the auto industry, for application in gas turbine engines that are particulate reinforced [8].

Even with this restriction a number of processing routes may be employed, and secondary processing may be applied to further tailor the material properties to meet a particular component requirement. The great advantage of particulate reinforcement, in terms of processing, is that conventional metal manufacturing methods and machining techniques can be used. This improves the economics of the case for the use of aluminium metal matrix composites relative to that of other composites, which have, traditionally, been expensive and very labour intensive [8].

CHAPTER 1. CLASSIFICATION OF METAL MATRIX COMPOSITES

1.1. Types of metal matrix composites

Metal matrix composites can be classified in various ways. One classification is the consideration of type and contribution of reinforcement components in particle-, layer-, fiber and penetration composite materials (see Fig. 1.1) [1]. Fiber composite materials can be further classified into continuous fiber composite materials (multi and monofilament) and short fibers or, rather, whisker composite materials, see Fig. 1.2. [1]

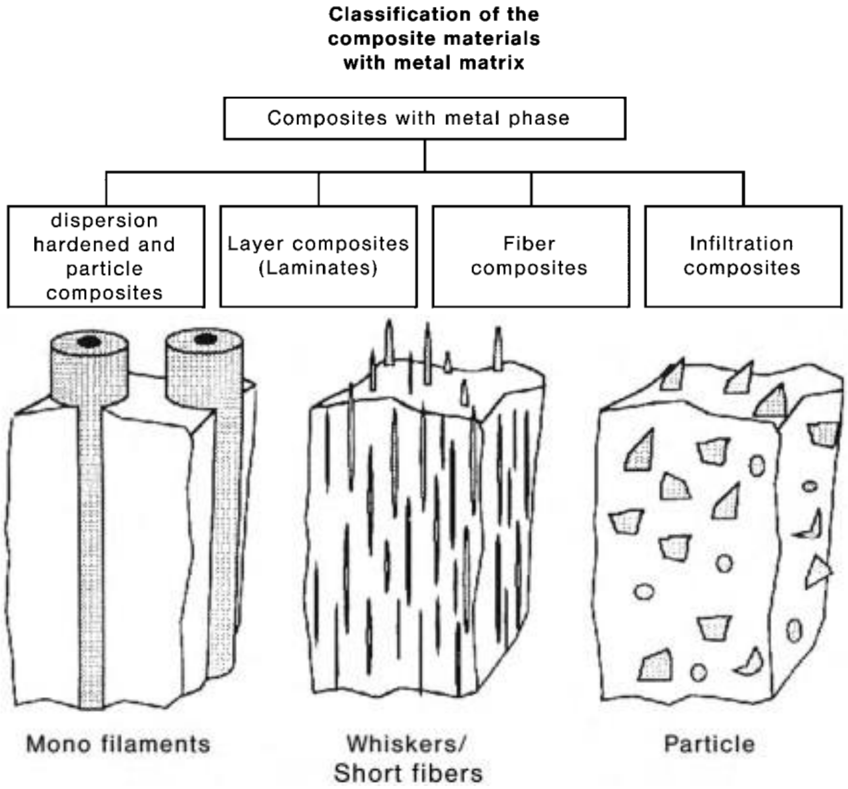

Figure 0.1. Classification of metal matrix composites [1]

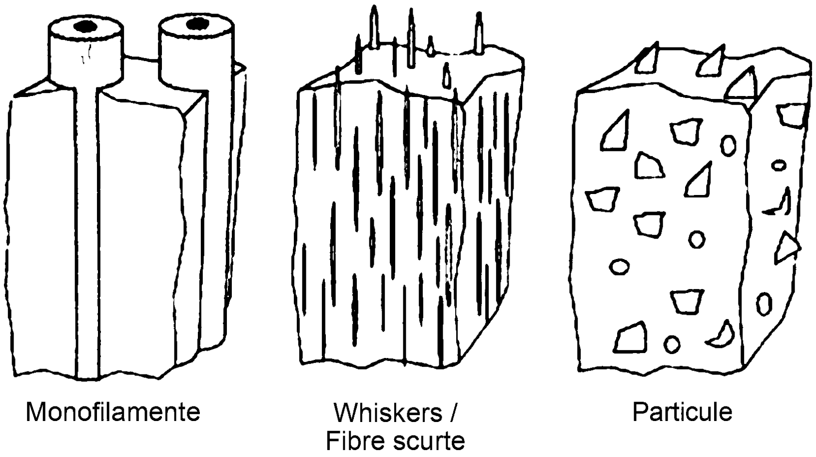

Figure 1.2. Schematic representation of three forms of metal matrix composites [1]

1.2. Reinforcement phases

Reinforcements for metal matrix composites have a manifold demand profile, which is determined by production and processing and by the matrix system of the composite material. The following demands are generally applicable [4]: [1]

- low density,
- mechanical compatibility (a thermal expansion coefficient which is low but adapted to the matrix),
- chemical compatibility,
- thermal stability,
- high Young’s modulus,
- high compression and tensile strength,
- good processability,
- economic efficiency. [1]

1.3. Particles, fibers and short fibers used for reinforcing metallic materials

The availability as well as the demand for reinforcing compounds for metal matrix composites is very extensive. Their selection depends on the condition of the matrix, the type of processing of the composite material and the demands on the material (temperature, corrosion, stress etc.). [1]

These demands can be almost exclusively fulfilled by nonmetal inorganic reinforcement components. Ceramic particles, or rather fibers or carbon fibers, are used for metal reinforcement. An application area of metal fibers is that of functional materials (for example for contacts, conductors and superconductors). However, their application in the structural area mainly fails because of the high density. Organic fibers cannot be employed because of their low Young’s modulus, processing problems, poor thermal stability and poor compatibility [12].

Reinforcement materials for metal matrix composites can be produced in the form of continuous fibers, short fibers, whiskers, or particles. The parameter that allows us to distinguish between these different forms of reinforcements is called the aspect ratio. Aspect ratio is nothing but the ratio of length to diameter (or thickness) of the fiber, particle, or whisker [13].

Thus, continuous fibers have an aspect ratio approaching infinity while perfectly equiaxed particles have an aspect ratio of around one.

Ceramic reinforcements combine high strength and elastic modulus with high temperature capability [13].

Continuous ceramic fibers are also, however, more expensive than ceramic particulate reinforcements [13].

Considering economic criteria, the use of discontinuous reinforcement, like particles or short fibers, appears most favorable [1].

CHAPTER 2. The study of the specialized literature

Numerous studies on the elaboration of aluminum matrix composite materials reinforced with ZrB_2, $ZrAl_3$ particles or containing both compounds, hybrid composites, are published in the specialized literature ($ZrB_2 + ZrAl_3$) [33 – 52].

Alloys A356 [33, 43, 46], AA6061 [35, 51, 52], AA2024 [36, 40], AA5052 [38, 39, 48], AA2618 [41], AA2014 [42] can be used as matrix material, AA6351 [44], AA7075 [47], AA6061 [47], A380 [50] or metallic aluminum: Al 99.7% powder [34], Al of purity over 98% [37, 45, 53 - 65] .

By reactions between aluminum alloys and Zr-containing elements (eg K_2ZrF_6) and boron-containing elements (eg KBF_4) [34, 37 - 48] or using Al-B and / or Al-Zr pre-alloys [33, 49], various concentrations of reinforcing elements were obtained, as final reaction products, intermediates or combinations thereof.

In addition to aluminothermic reactions, other methods were used such as borothermic and carbothermic reduction, mechanochemical treatment, CVD, sol-gel, thrombolysis of ZrB_2-containing gas, magnetochemical process, etc. [53 - 65].

The main diagram studied was that of Al - K_2ZrF_6 - KBF_4, but studies were also presented on the binary diagrams KF-NaF, KF-KCl, KCl-NaCl [53 - 65], following the melting temperatures at various concentrations, so that the salts are in the liquid state for the best possible conditions for the development of the formation reactions of the reinforcing compounds.

A very important parameter when obtaining metal matrix composites reinforced with Al_3Zr, ZrB_2 etc. was the working temperature. Thus, from the study of the literature it results that we must have temperatures higher than 700°C [5]: 850°C [33, 42, 44, 47, 49], 860°C [39], 870°C [36, 40], 885°C [38, 48], 900°C [44]. In the study [44], the authors performed the analysis of the compound $ZrAl_3$ and its morphology at 850°C, 900°C, 950°C and 1000°C.

Another parameter that has an influence both on the process of obtaining composite materials and on the quantity and dimensions of the reaction products, is the stirring time of the mixture formed by the liquid matrix material and the salts used for the addition of B and Zr. Stirring times varied with values ranging from 10 minutes [49], 20 minutes [42], 30 minutes [44, 48], 40 minutes [47], exceeding one hour or reaching up to 4 hours [34].

As a result of the reactions, reinforcing particles with different morphologies were obtained, with dimensions starting from 15 nm [36, 39, 40] and reaching 100 μm [33, 46, 50, 52].

Samples from the composite materials obtained were analyzed by optical microscopy - MO [35, 36, 40, 42, 44, 47 - 50] and SEM and TEM electron microscopy [33 - 40, 43 - 52], as well as X-ray diffraction (XRD), as can be seen in the following figures (2.1 - 2.5).

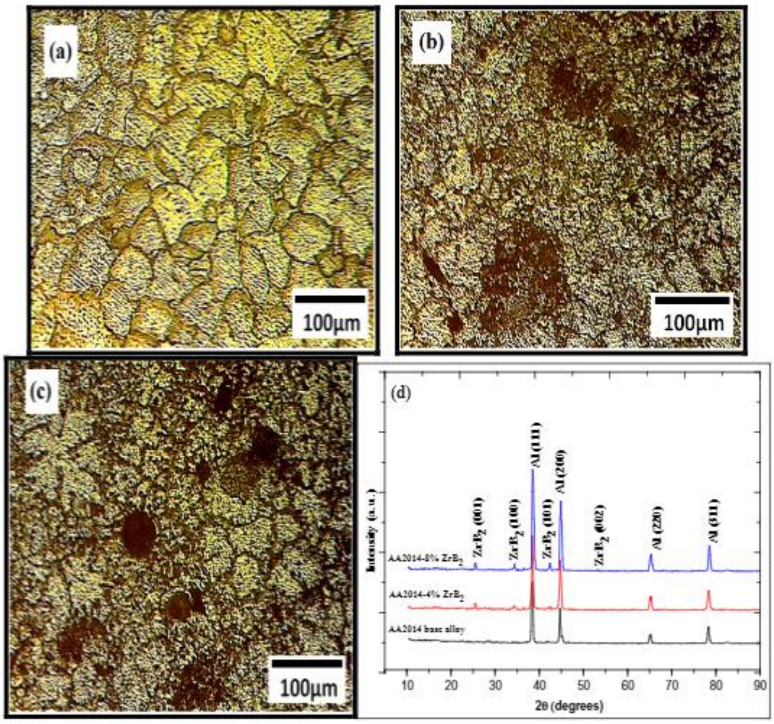

Figure 2.1. Optical microscopy of AA2014 (a) alloy, AA2014 / 4% ZrB_2 (b) composite AA2014 / 8% ZrB_2 (c) composite, and XRD for AA2014 / ZrB_2 (d) composite [42]

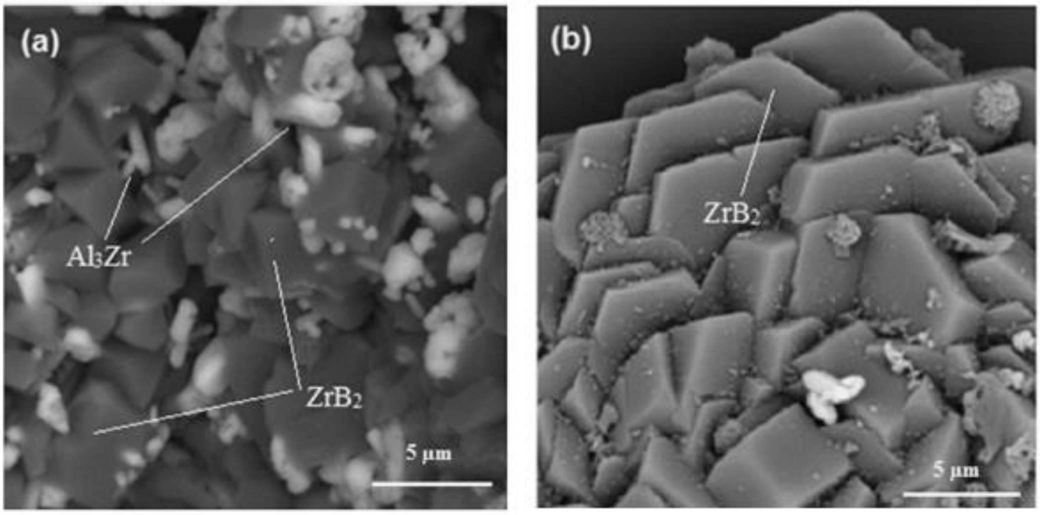

Figure 2.2. SEM microstructures of particles extracted from the composite material, obtained at 600°C (a) and 800°C (b), reaction time 2 hours [34]

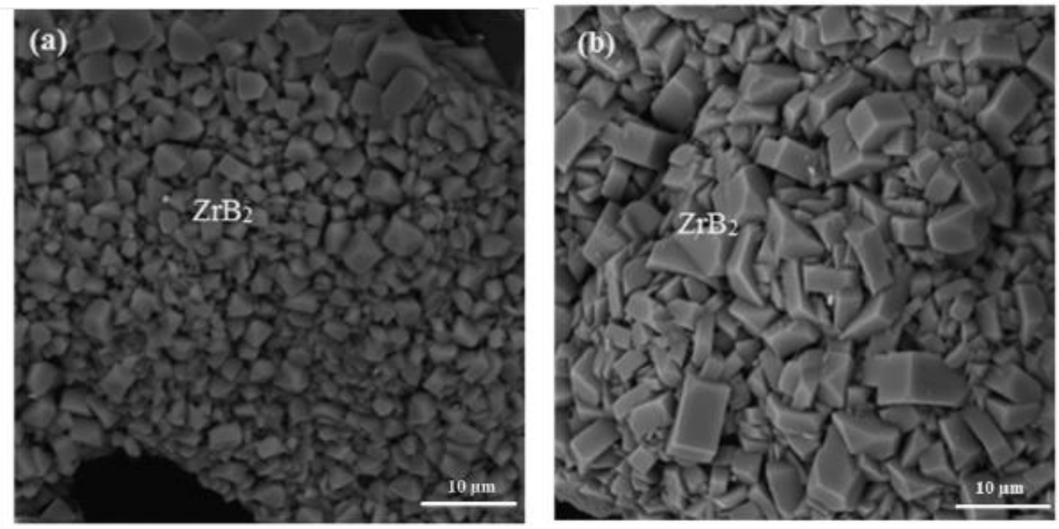

Figure 2.3. SEM microstructures of particles extracted from the composite material obtained at 800oC, reaction time 1 hour (a) and 2 hours (b) [34]

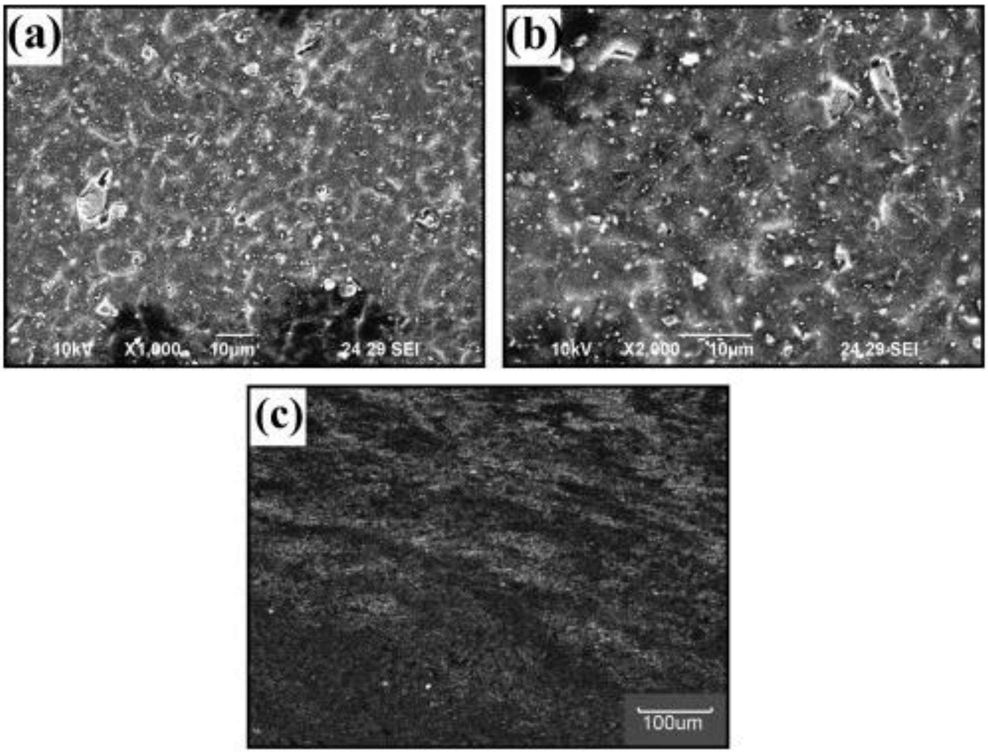

Figure 2.4. SEM microstructures (a, b) and optical microstructure of composite AA6061 / Al_3Zr [35]

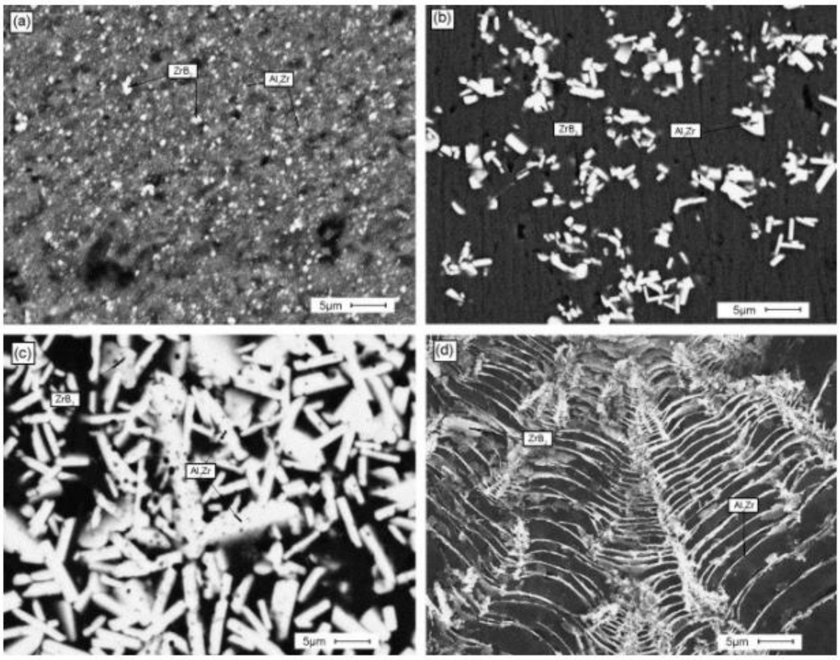

Figura 2.5. Imagini SEM ale compozitelor Al/Al_3Zr + ZrB_2 obținute la diferite temperaturi: (a) 1123 K; (b) 1173 K; (c) 1223 K și (d) 1273 K [45]

Other techniques for highlighting the structures and compounds formed are: XRF [34], XRD and EDAX [35, 36, 37, 39, 40, 42 - 52], DTA-TG [37], TEM [33, 36, 39, 40], HRTEM [34, 36]. The properties of the obtained materials were subjected to tests to determine the physical-mechanical properties (hardness, wear resistance, mechanical strength, elongation, expansion) [33, 38, 39, 40, 42 - 50], to determine the corrosion potential, the currents of corrosion, linear polarization resistance, etc. [41].

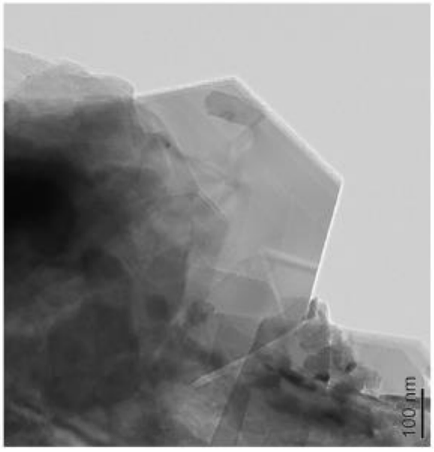

Figure 2.6. TEM image for ZrB_2 compound, obtained at 800oC, reaction time 2 hours [34]

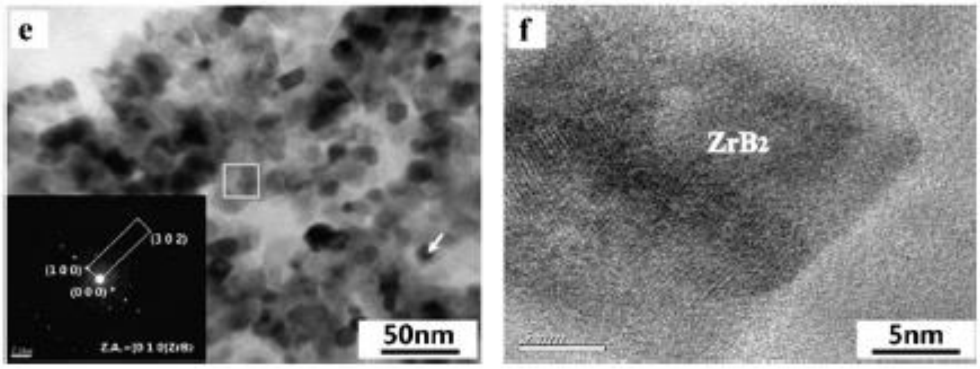

Figure 2.7. TEM image (s) with highlighting reinforcement elements and HRTEM image (f) of the shaded area with white square (s) [36]

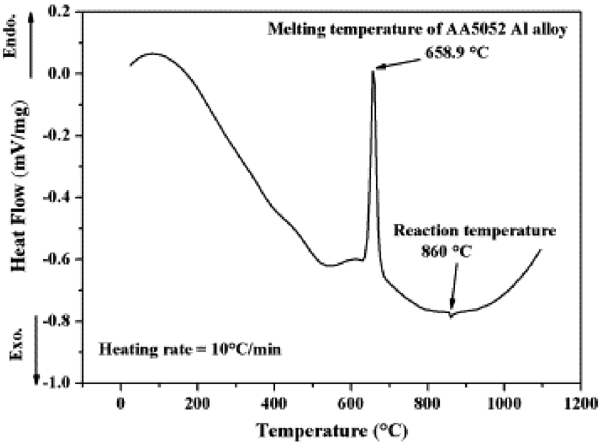

Figure 2.8. Thermogravimetric analysis for composite AA5052 / ZrB_2 [36]

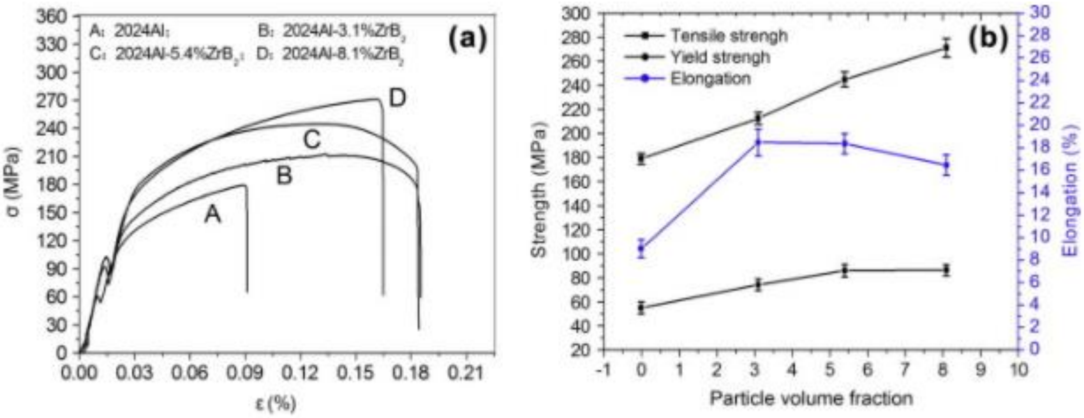

Figure 2.9. Determined mechanical properties for AA2024 / ZrB_2 composite [40]

CHAPTER 3. Studies and research on the thermodynamics of in situ processes of obtaining Al matrix composites reinforced with ZrB_2 particles

Studies and research on the in-situ production of aluminum matrix composites and reinforcing particles in the form of boron are presented in the literature. However, there is no unitary view of the thermodynamics of the interaction processes of aluminum alloys introduced into the melt with KBF_4 and K_2ZrF_6 salts at high temperatures. The addition of salts in molten aluminum, at 890°C, generates the intermetallic compounds Al_3Zr and AlB_2 in the first phase and, after the completion of the reaction, the compound ZrB_2. In order to clarify the evolution of the in situ reaction, thermodynamic calculations of the reactions proposed by different authors were performed using the HSC Chemistry 6.0 program.

According to the thermodynamic studies of Degang Zhao et al. [66], the total ZrB_2 formation reaction by the interaction between pure Al (99.85% wt.) and salts, at 1173K is (3.1), having the free energy of negative Gibbs formation ($\Delta G = -758.73$ kJ / mol).

$$K_2ZrF_6 + 2\ KBF_4 + 10/3\ Al = ZrB_2 + 10/3\ AlF_3 + 4\ KF \qquad (3.1)$$

For calculations according to the HSC Chemistry 6.0 program, K_2ZrF_6 was considered dissociated into ZrF_4 and 2KF.

$$ZrF_4 + 2\ KF + 2\ KBF_4 + 10/3\ Al = ZrB_2 + 10/3\ AlF_3 + 4\ KF \qquad (3.2)$$

In table 3.1. the results of the thermodynamic calculation for this reaction are presented again in (Figure 3.1) Ellingham diagram.

Table 3.1. The result of the thermodynamic calculation of the reaction (3.2)

$ZrF_4 + 2\ KF + 2\ KBF_4 + 10/3\ Al = ZrB_2 + 10/3\ AlF_3 + 4\ KF$					
T, °C	deltaH, kJ	deltaS, J/grad	deltaG, kJ	K	Log(K)
700	-917,920	-272,888	-652,359	1,044E+035	35,019
720	-918,961	-273,947	-646,891	1,062E+034	34,026
740	-919,985	-274,967	-641,402	1,178E+033	33,071
760	-920,990	-275,950	-635,892	1,421E+032	32,153
780	-921,978	-276,897	-630,364	1,852E+031	31,268
800	-922,947	-277,809	-624,817	2,600E+030	30,415
820	-923,898	-278,687	-619,252	3,914E+029	29,593
840	-924,831	-279,533	-613,669	6,294E+028	28,799
860	-871,336	-232,198	-608,220	1,095E+028	28,039
880	-872,128	-232,891	-603,569	2,200E+027	27,342
900	-872,916	-233,569	-598,905	4,662E+026	26,669
920	-934,702	-285,798	-593,703	9,858E+025	25,994
940	-935,477	-286,441	-587,981	2,084E+025	25,319
960	-936,233	-287,060	-582,245	4,626E+024	24,665
980	-936,972	-287,654	-576,498	1,077E+024	24,032

K - the equilibrium constant of the reaction

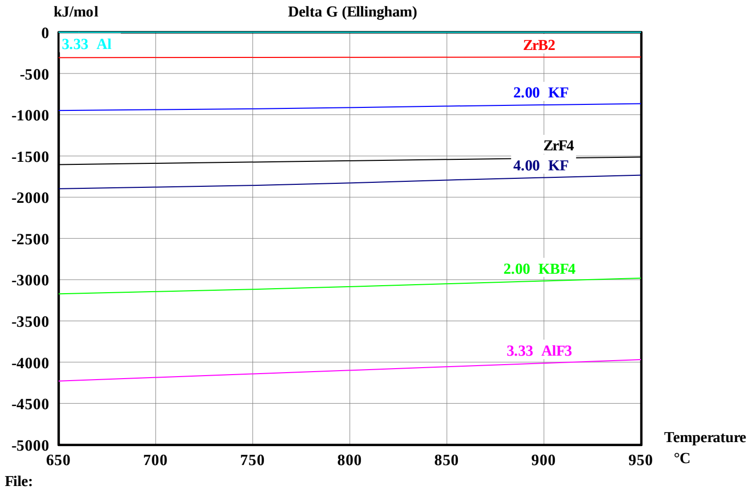

Figure 3.1. Ellingham diagram ΔG^o_T = f(T) for the formation of molten ZrB_2 (reaction 3.2)

In figure 3.2. the variation of the thermodynamic parameters of the reaction is given 3.2.

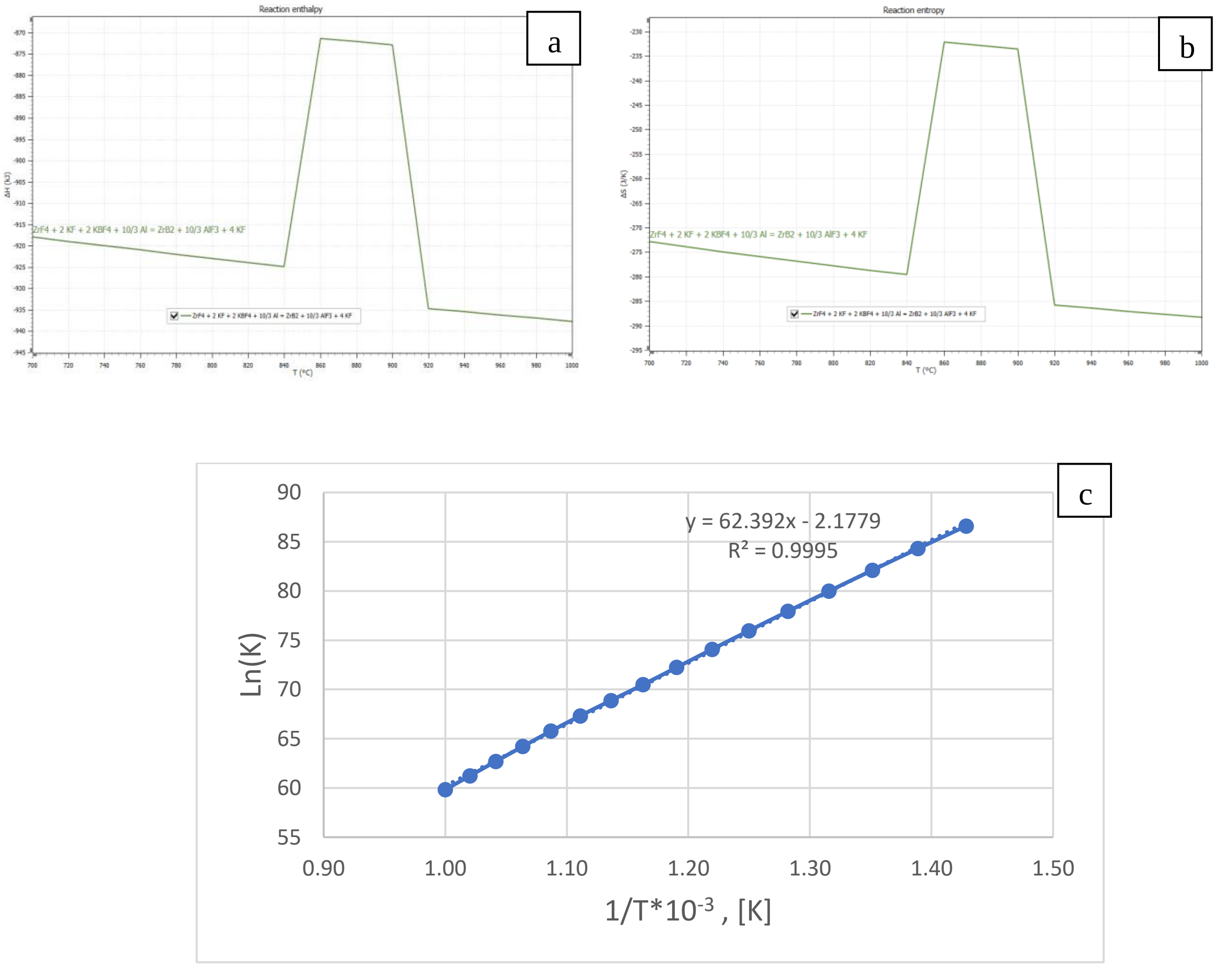

Figure 3.2. Variation of the thermodynamic parameters of the reaction (3.2): a) enthalpy variation; b) entropy variation; c) variation ln K = f (1 / T)

In conclusion, the reaction 3.1. it is thermodynamically possible having a negative ΔG at 1173K (900°C).

CHAPTER 4. Development of AA6063 / ZrB_2 composites by in situ reactions

The literature presents a series of studies on obtaining aluminum matrix composites of series AA7075, A356, AA2024, AA5052, AA2014, AA6061, reinforced with zirconium diboride particles, obtained by aluminothermic reactions at different temperatures (1000 K, 1023 K, 1123 K, 1143 K, 1158 K, 1163 K 1173 K) using different concentrations of KBF_4 (for B) and K_2ZrF_6 (for zirconium) salts.

In Chapter 3 of this doctoral dissertation, determinations were made using the HSC Chemistry 6.0 program regarding the thermodynamics of in situ reactions in order to obtain ZrB_2 particles, for the temperature range 700 - 1000^oC.

It was concluded that reaction 3.13 has the highest values in the studied temperature range, for the free energy of Gibbs formation.

$$6KF + 3ZrF_4 + 6KBF_4 + 10Al = 3ZrB_2 + 9KAlF_4 + K_3AlF_6 \qquad (3.13)$$

The aluminothermic reaction for the formation of zirconium diboride can be carried out in several stages, the first of which being to obtain aluminium diboride, according to reaction 3.7.

$$6\ KBF_4 + 9\ Al = 3\ AlB_2 + 2\ K_3AlF_6 + 4\ AlF_3 \qquad (3.4)$$

followed by obtaining the zirconium aluminide ($ZrAl_3$) according to reaction (3.4)

$$6\ K_2ZrF_6 + 13\ Al = 3\ Al_3Zr + 2\ K_3AlF_6 + 2\ AlF_3 \qquad (3.7)$$

și ulterior, în urma reacției dintre AlB_2 și $ZrAl_3$, cu formarea diborurii de zirconiu, conform reacției (3.8).

$$ZrAl_3 + AlB_2 = ZrB_2 + 4Al \qquad (3.8)$$

In the present doctoral thesis we aimed to obtain by aluminothermic reactions, composites with AA6063 alloy matrix reinforced in situ with zirconium diboride particles.

For the study it was desired to obtain composites with different concentrations of reinforcing materials (2.5% ZrB_2, 5% ZrB_2, 7.5% ZrB_2, 10% ZrB_2) at a temperature of 900^oC.

4.1. The technological flow of in situ elaboration of composites and the experimental procedure

The in situ technological flow of Al / ZrB_2 composites

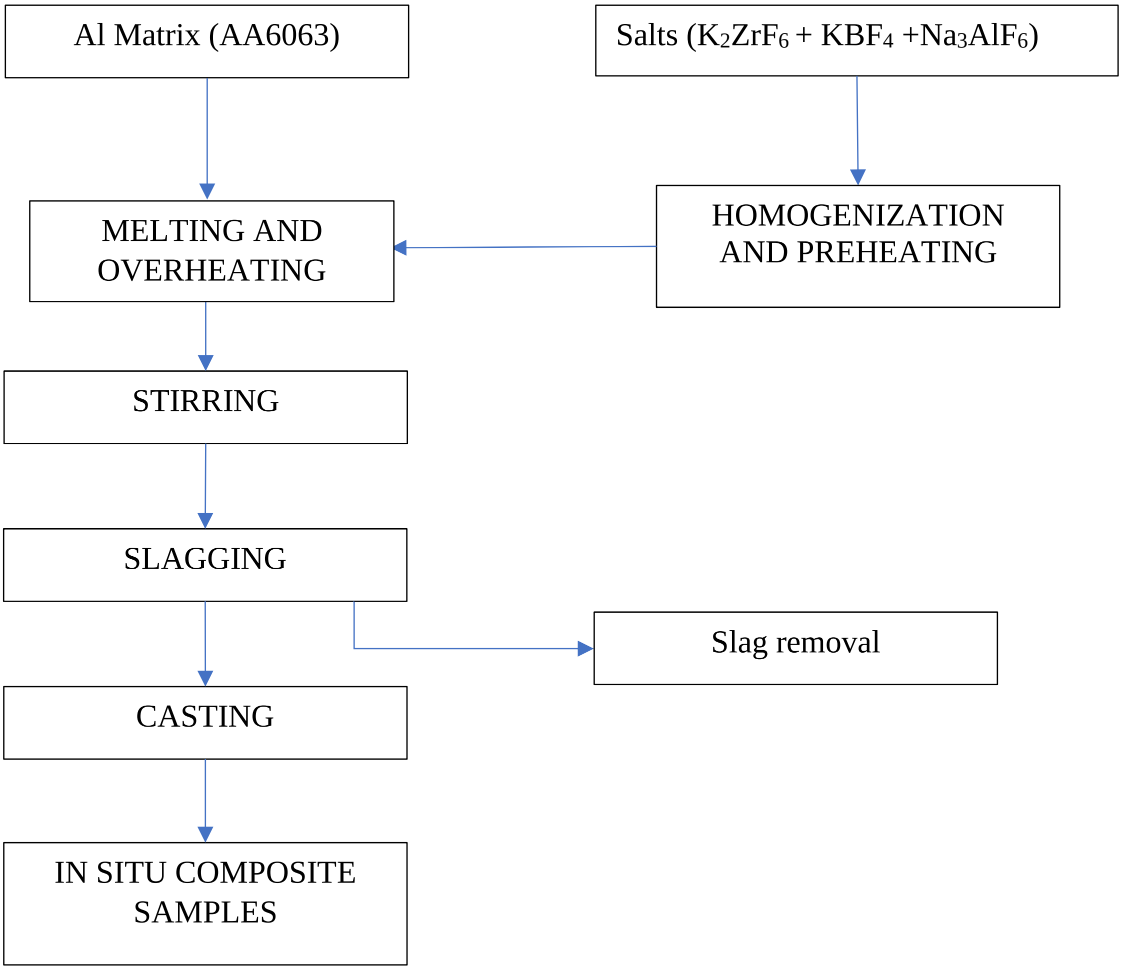

Figure 4.1. Schematic of the technological process of in situ elaboration of Al / ZrB_2 composites

4.2. Load calculation

The amounts of K_2ZrF_6 and KBF_4 were calculated according to the reactions below, in order to determine the salt required to obtain boron-containing composites in amounts of 7.5, 15, 22.5, 30 g of ZrB_2, per 300 g of alloy used according to the general reaction to obtain composite materials (3.13):

$$3K_2ZrF_6+6KBF_4+10Al = 3ZrB_2 + 9KAlF_4 + K_3AlF_6+ \qquad (3.13)$$

The bars were cast in a preheated steel shell at 200°C (Figure 4.2.)

Figure 4.2. AA6063 / ZrB_2 composite cast bars

Samples were taken from the samples obtained for the characterization from a compositional point of view and the characterization of the physical-mechanical properties. The notations of the samples are: A (2.5% ZrB_2); B (5% ZrB_2); C (7.5% ZrB_2); D (10% ZrB_2).

The samples were processed by metallographic methods (cutting with the DELTA Abrasimet device, bakelite embedding with the SIMPLIMET 1000 device, polishing and sanding with the Buehler Beta / 1 Single device) and subsequently analysed by optical microscopy using the Olympus BX51M Optical Microscope with Olympus U30 camera and Olympus Stream Essentials software. The samples were attacked with Keller reagent (95 ml H_2O, 2.5 ml HNO_3, 1.5 ml HCl and 1 ml HF).

The presence of the present reinforcement phases was confirmed by electron microscopy using the SEM FEI Quanta Inspect F field emission microscope and equipped with an energy dispersion spectrometer (EDS).

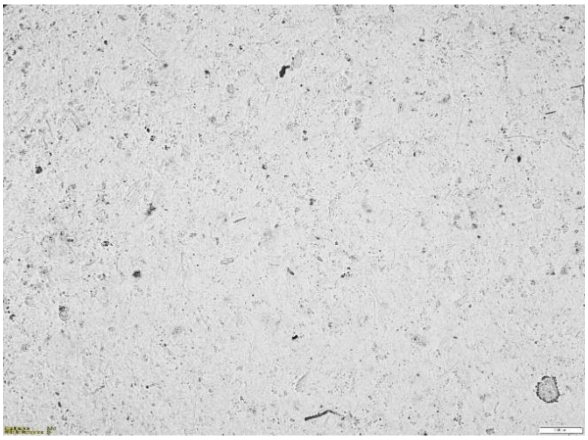

A attacked zone 1 x50

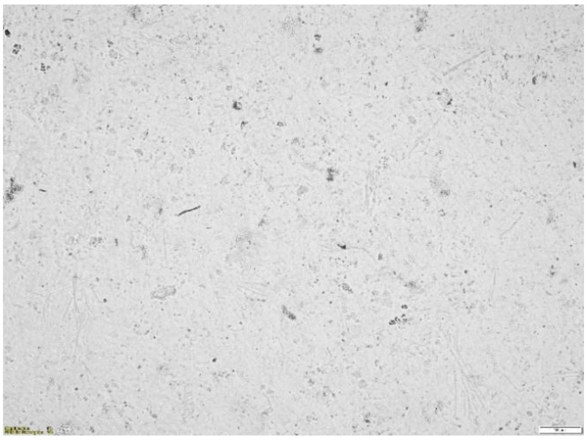

A attacked zone 1 x100

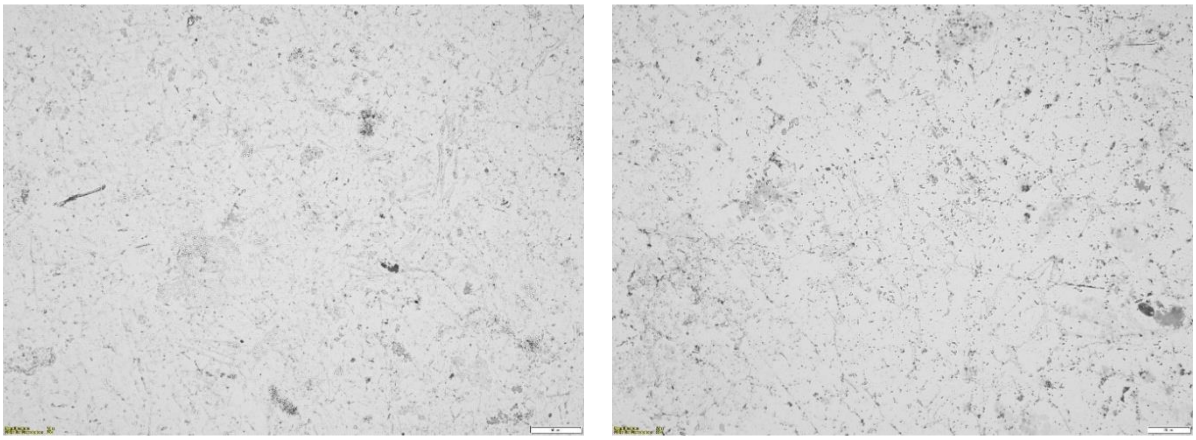

A attacked zone 1 x200 A attacked zone 1 x500

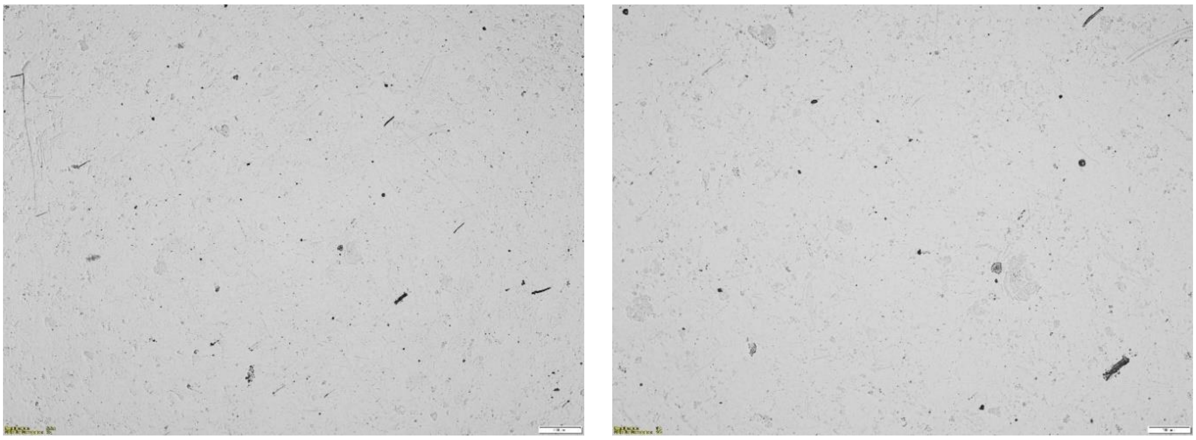

A unattacked zone 1 x50 A unattacked zone 1 x100

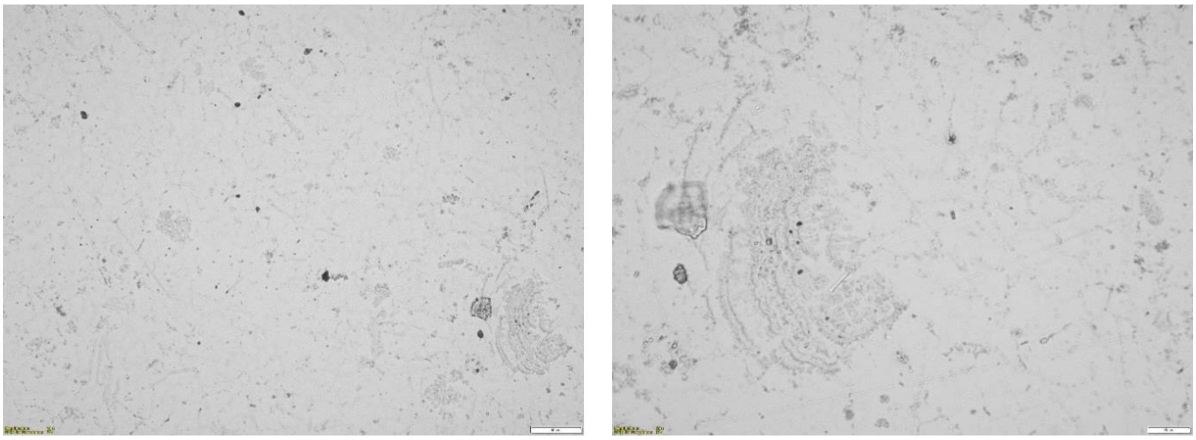

A unattacked zone 1 x200 A unattacked zone 1 x500

Figure 4.3. The microstructure of composite A attacked and unattacked on different areas and sizes

The SEM micrograph of the AA6063 matrix and the EDS analysis of the AA6063 / ZrB_2 composite is shown in Figure 4.4.

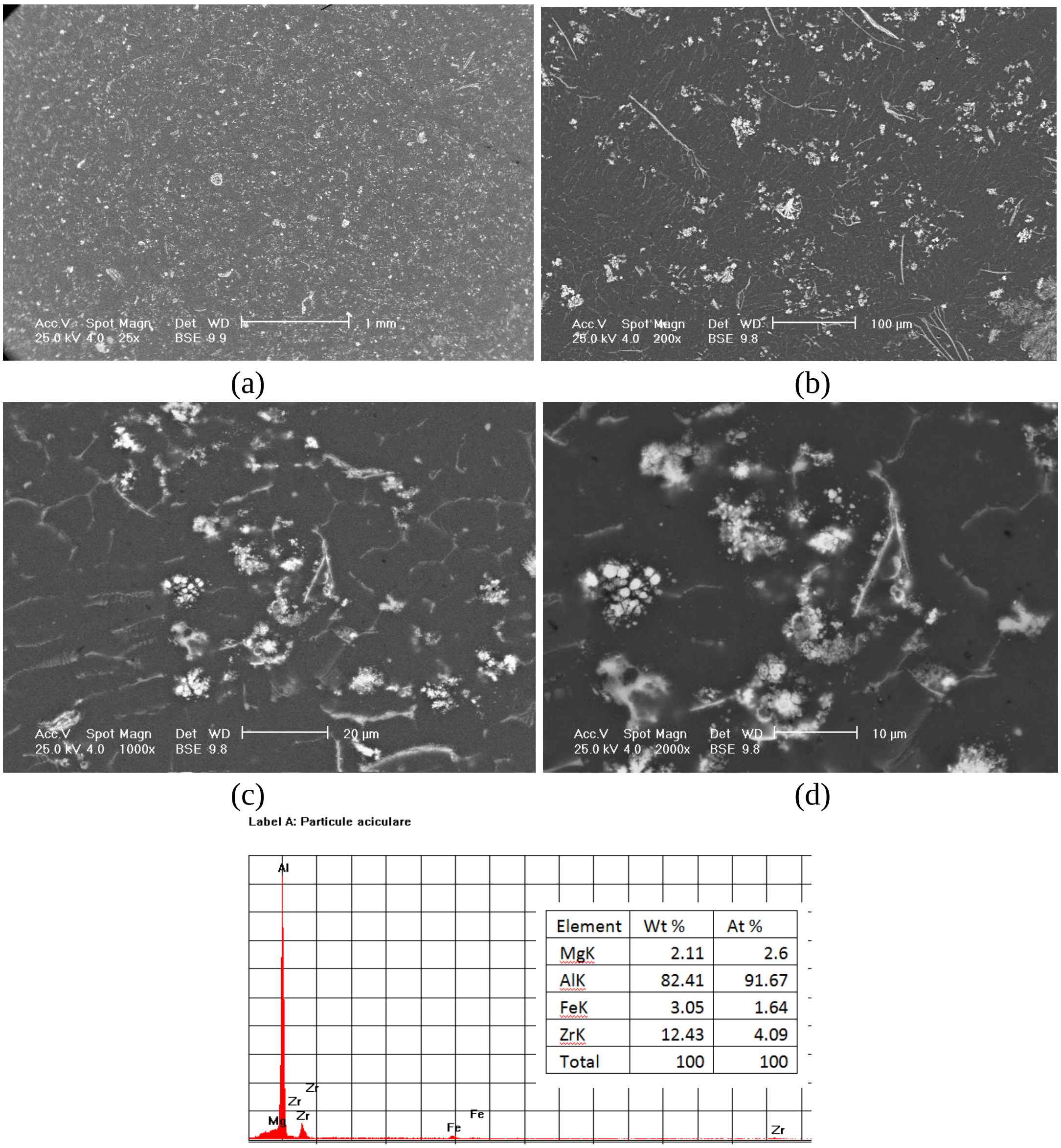

(a) (b)

(c) (d)

Element	Wt %	At %
MgK	2.11	2.6
AlK	82.41	91.67
FeK	3.05	1.64
ZrK	12.43	4.09
Total	100	100

Figure 4.4. SEM analysis of matrix AA6063 (a), composites AA6063 / ZrB_2 (b, c, d) with 2.5% ZrB_2 and EDS analysis with chemical composition of sample A

The microstructure of the matrix alloy is typically dendritic. The completely dendritic microstructure is absent in the composites, confirming the finishing of the granulation by the fine particles of ZrB_2 and $TiAl_3$ (Figure 4.4.) Which act as granulation finishers. Figure 4.5 shows the microstructures of the attacked and unattacked sample D. In some areas the formation of ZrB2 clusters is observed.

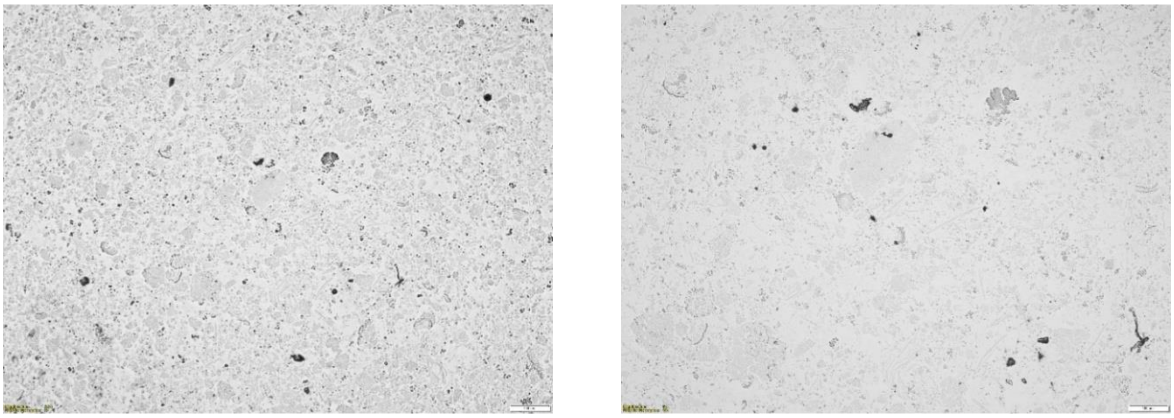

D attacked zone 1 x50 D attacked zone 1 x100

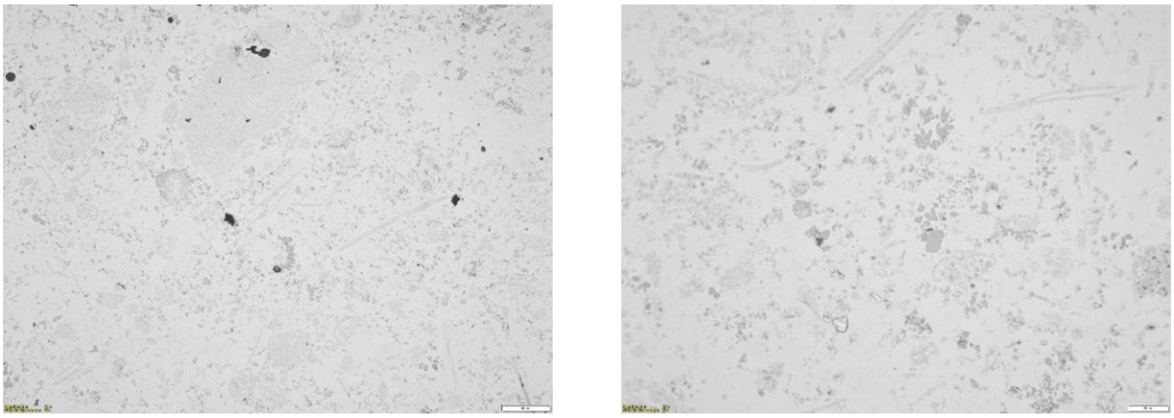

D attacked zone 1 x200 D attacked zone 1 x500

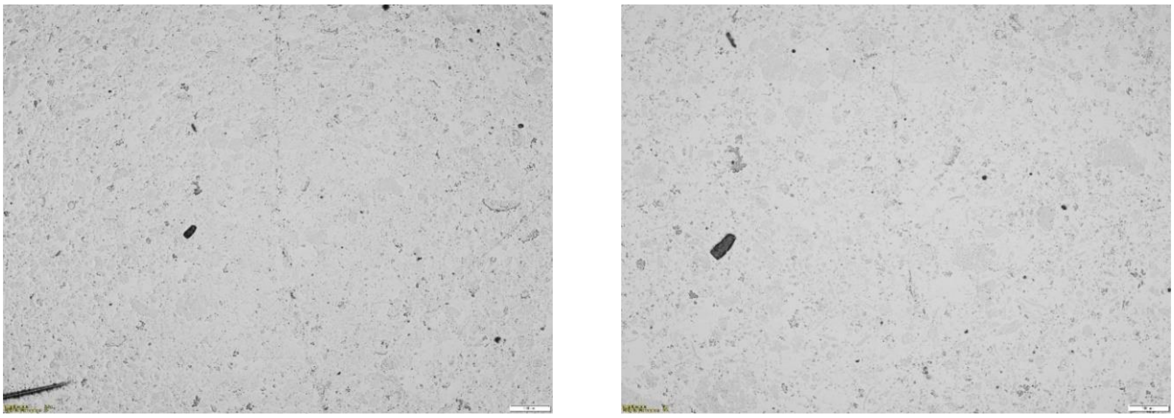

D unattacked zone 1 x50 D unattacked zone 1 x100

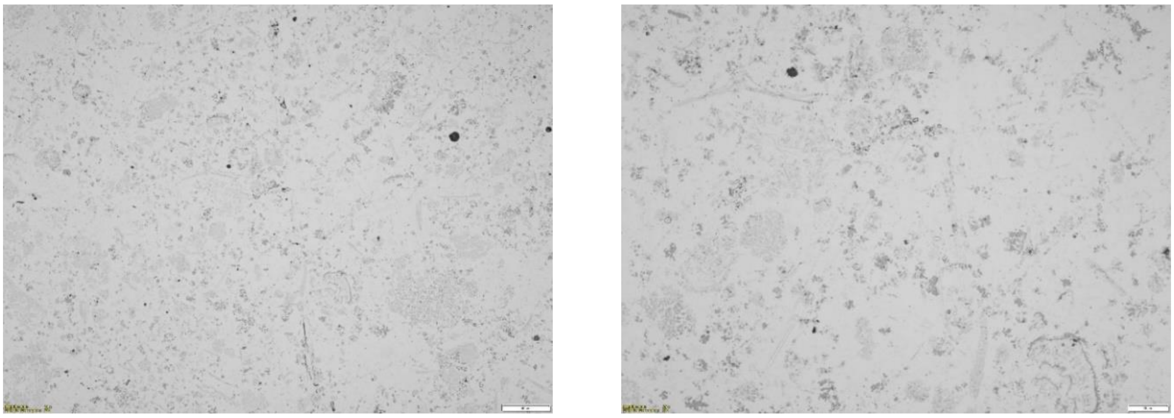

D unattacked zone 1 x200 D unattacked zone 1 x500

Figure 4.5. Microstructure of composite D unattacked and attacked, at different magnifications and in different areas

In Figure 4.6. the SEM analysis of composite D is presented as well as the EDS analysis of Zr-containing particles. The 10% increase in ZrB_2 particles leads, in some areas, to their agglomeration (Figure 4.6 c).

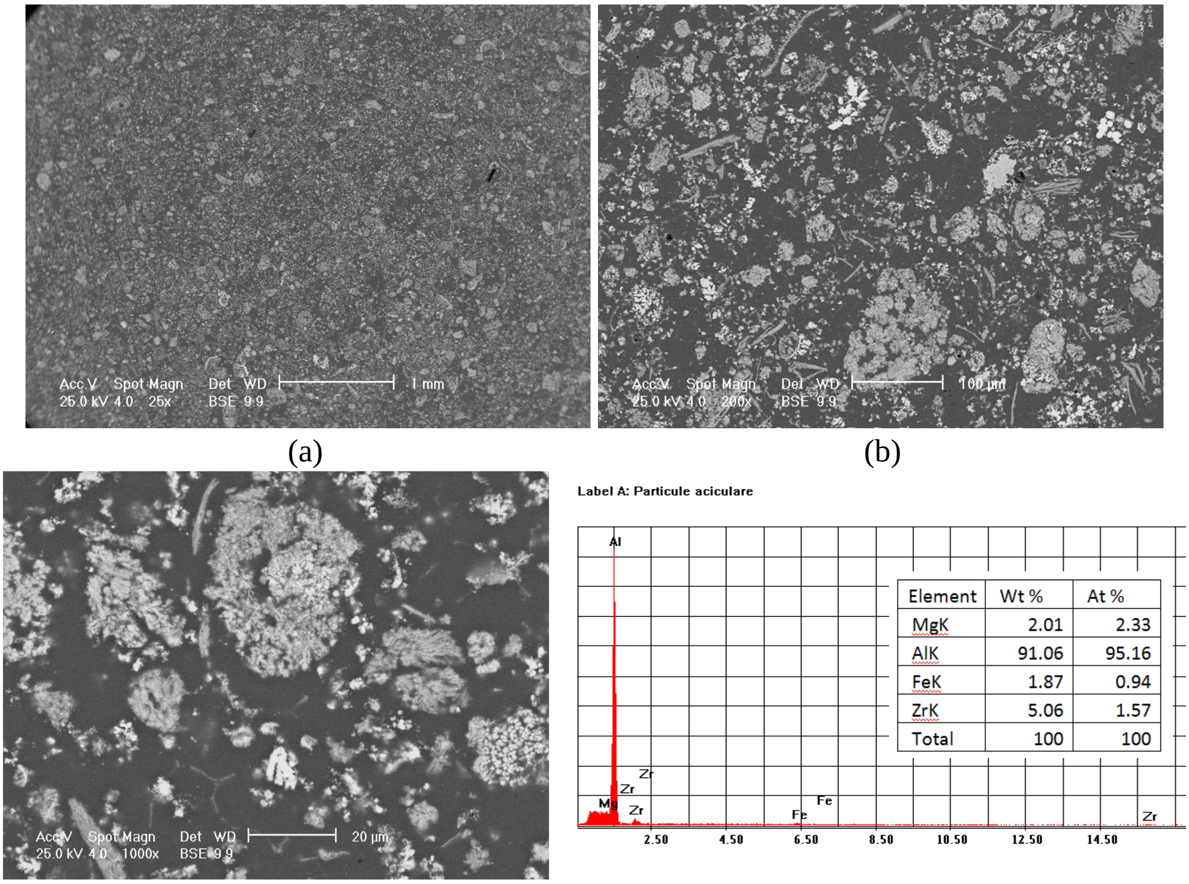

Element	Wt %	At %
MgK	2.01	2.33
AlK	91.06	95.16
FeK	1.87	0.94
ZrK	5.06	1.57
Total	100	100

(a) (b)

(c) (d)

Figure 4.6. ME analysis and EDS analysis with the chemical composition of sample D

XRD analysis of samples at different concentrations of ZrB_2 was performed with the PANalytical X'Pert PRO diffractometer (Figure 4.7 - Figure 4.10) but also with the D8 ADVANCE diffractometer (Figure 4.11).

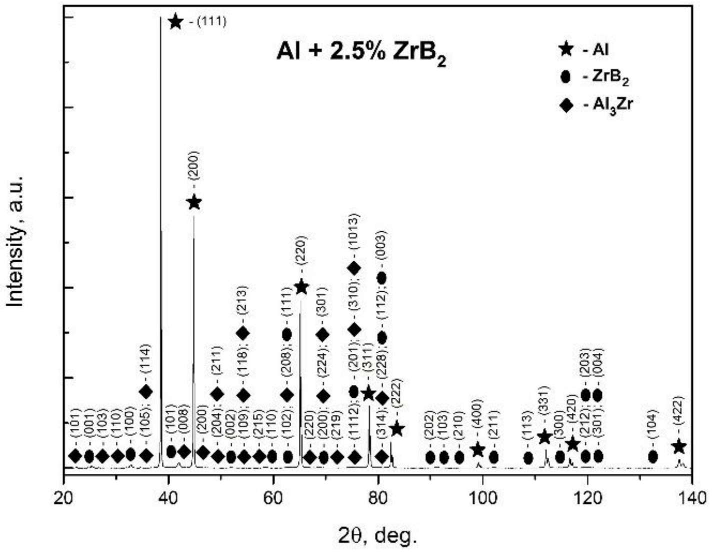

Figure 4.7. XRD AA6063 / 2,5% ZrB_2

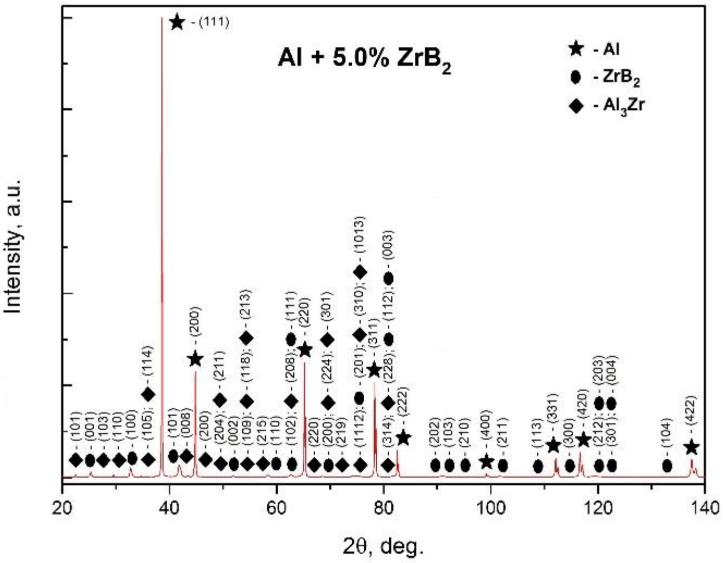

Figure 4.8. XRD AA6063 / 5,0% ZrB_2

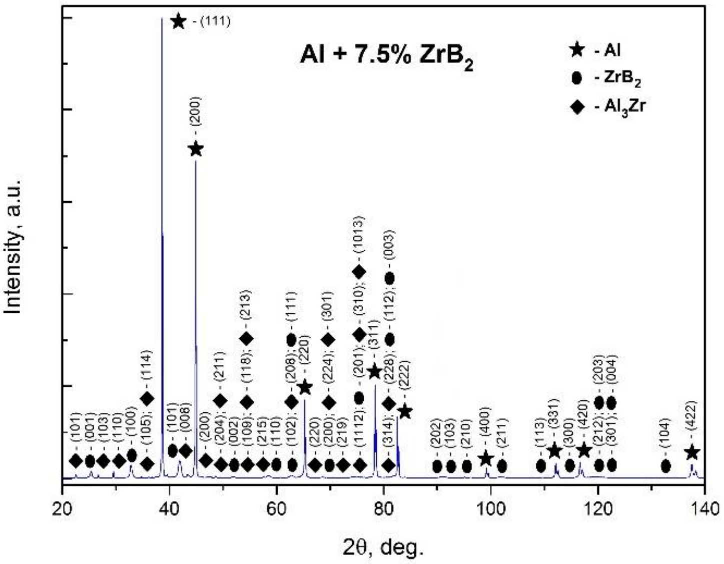

Figure 4.9. AA6063 / 7,5% ZrB_2

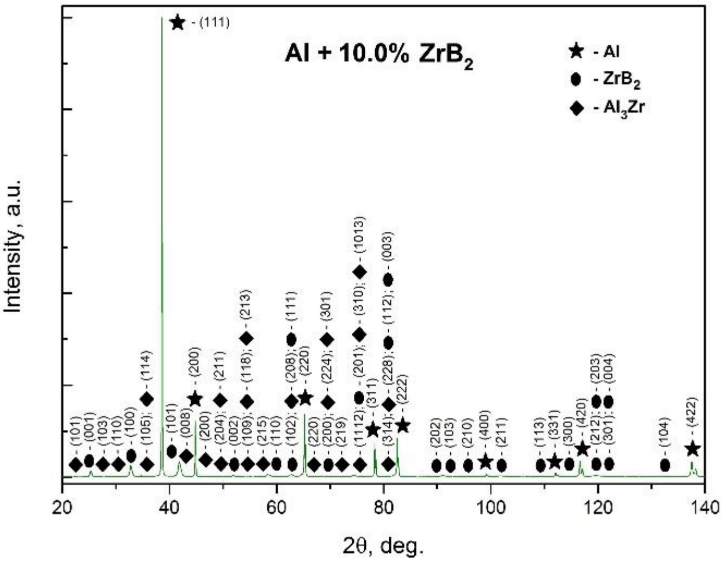

Figure 4.10. AA6063 / 10,0% ZrB_2

It was highlighted that all samples of composite materials contain ZrB2, Al_3Zr and Al.

The ADVANCE D8 diffractometer is based on the unique platform of the D8 family of diffractometers and is perfectly designed for all X-ray and dispersion diffraction applications, including:

- X-ray diffraction (XRD)
- Pair distribution function (PDF analysis)
- Wide and small angle X-ray scattering (SAXS, WAXS)

D8 ADVANCE has the ability to measure all types of samples, from liquids to free powders, from thin films to solid blocks, on a single instrument [80].

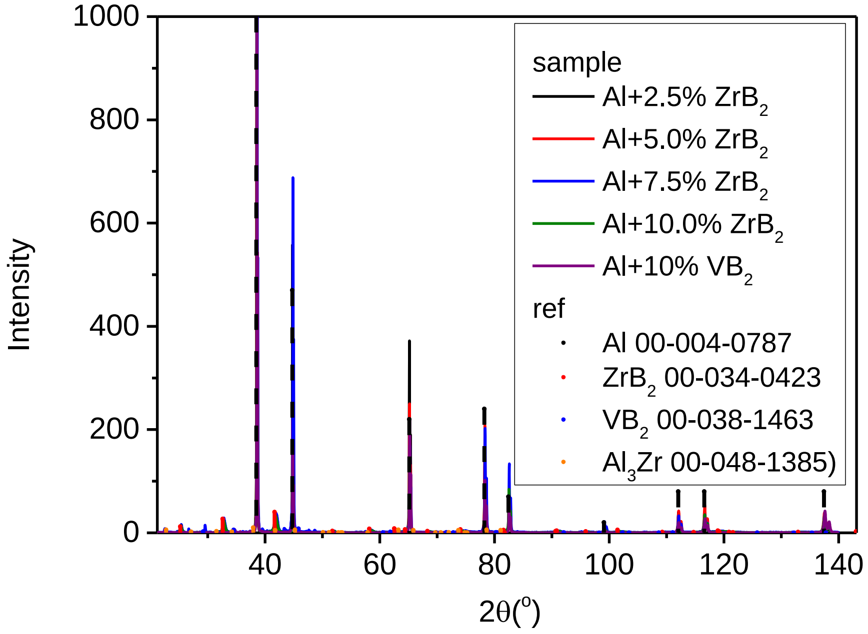

(a)

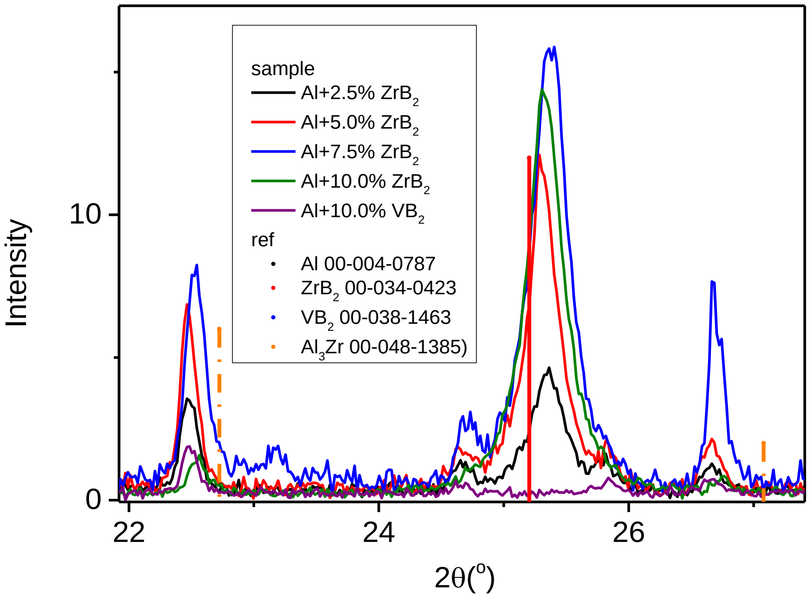

(b)

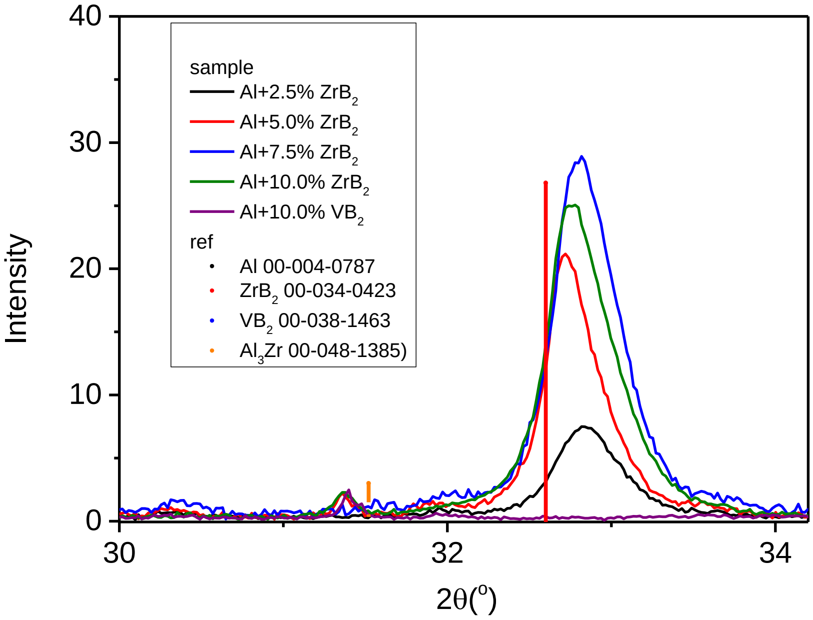
40
30
20
10
0
Intensity
30
32
34
2θ(°)
sample
Al+2.5% ZrB2
Al+5.0% ZrB2
Al+7.5% ZrB2
Al+10.0% ZrB2
Al+10.0% VB2
ref
Al 00-004-0787
ZrB2 00-034-0423
VB2 00-038-1463
Al3Zr 00-048-1385)

(d)

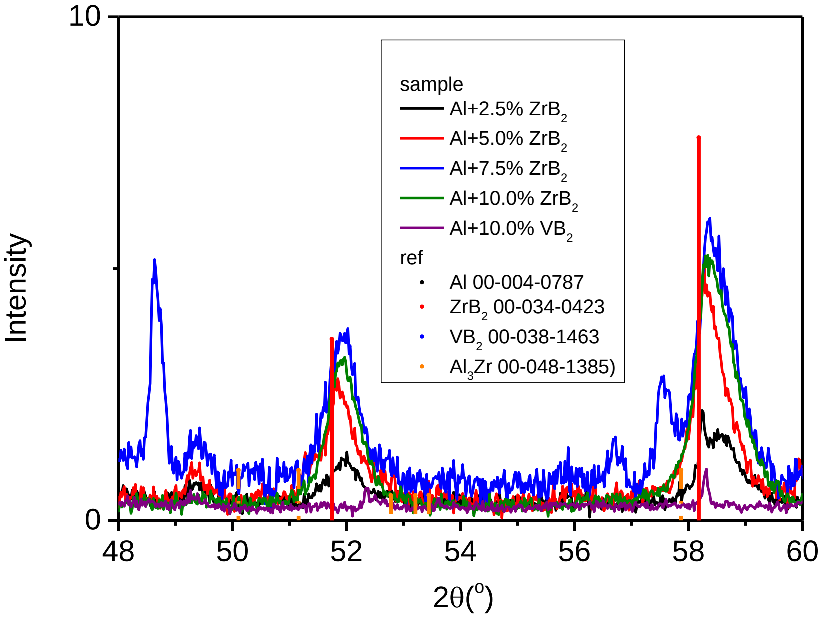
10
0
Intensity
48
50
52
54
56
58
60
2θ(°)
sample
Al+2.5% ZrB2
Al+5.0% ZrB2
Al+7.5% ZrB2
Al+10.0% ZrB2
Al+10.0% VB2
ref
Al 00-004-0787
ZrB2 00-034-0423
VB2 00-038-1463
Al3Zr 00-048-1385)

(f)

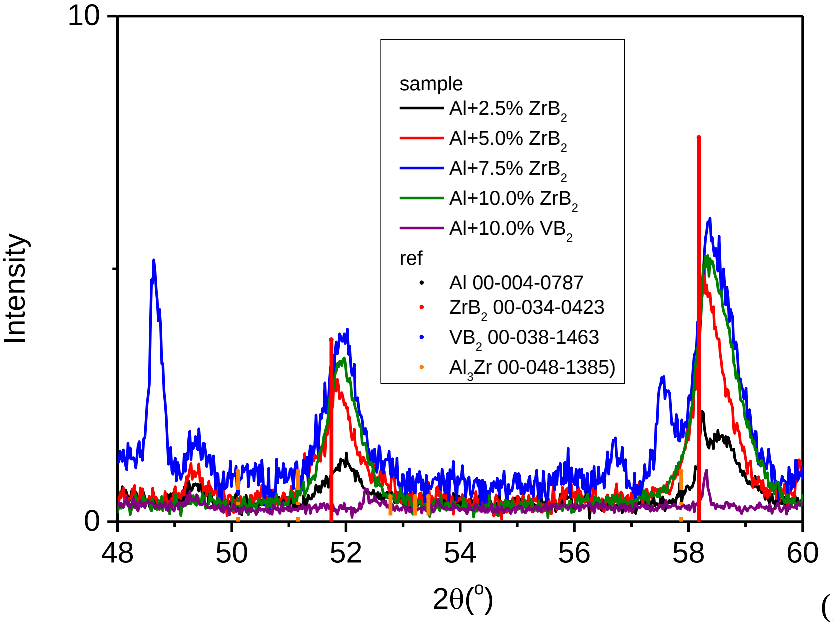
10
0
Intensity
48
50
52
54
56
58
60
2θ(°)
sample
Al+2.5% ZrB2
Al+5.0% ZrB2
Al+7.5% ZrB2
Al+10.0% ZrB2
Al+10.0% VB2
ref
Al 00-004-0787
ZrB2 00-034-0423
VB2 00-038-1463
Al3Zr 00-048-1385)

(g)

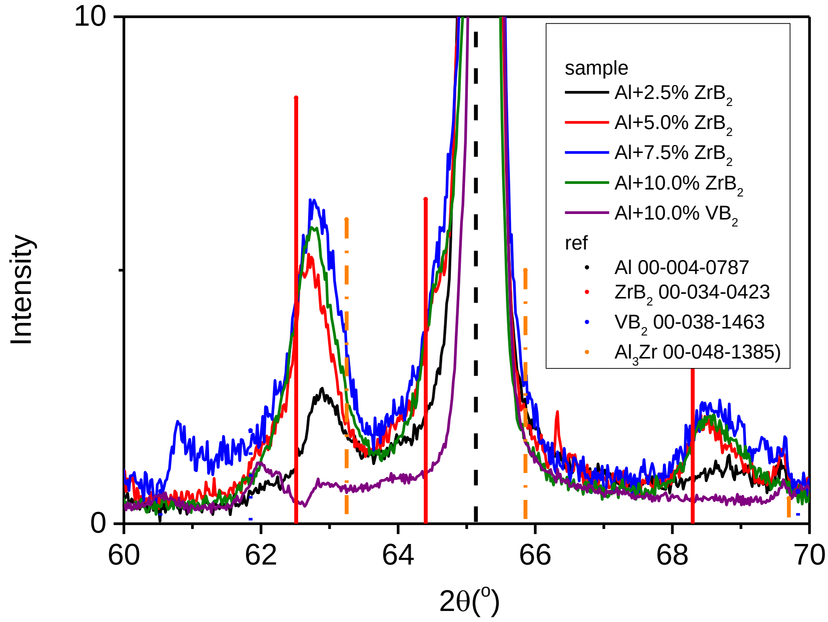

Intensity
2θ(°)
10
0
60
62
64
66
68
70
sample
Al+2.5% ZrB_2
Al+5.0% ZrB_2
Al+7.5% ZrB_2
Al+10.0% ZrB_2
Al+10.0% VB_2
ref
Al 00-004-0787
ZrB_2 00-034-0423
VB_2 00-038-1463
Al_3Zr 00-048-1385)

(h)

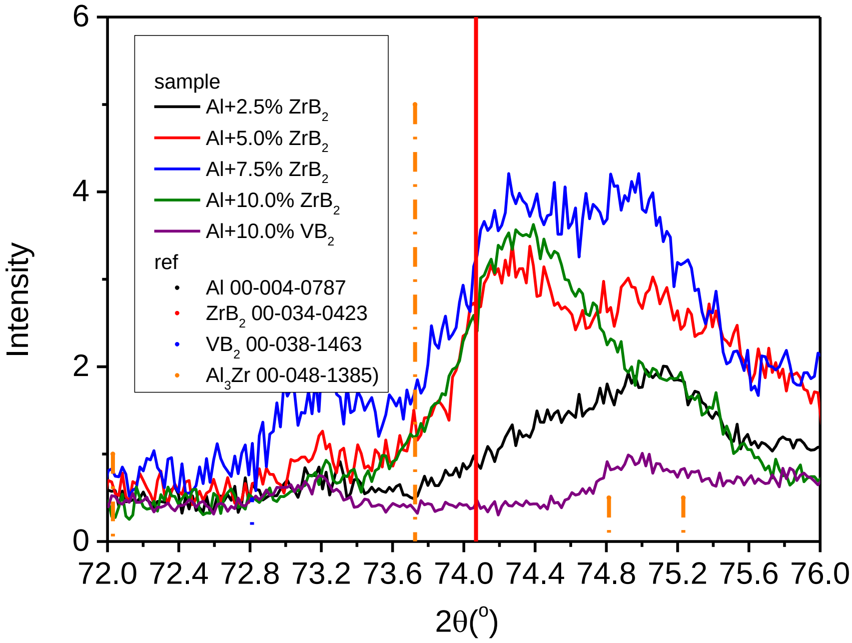

Intensity
2θ(°)
6
4
2
0
72.0
72.4
72.8
73.2
73.6
74.0
74.4
74.8
75.2
75.6
76.0
sample
Al+2.5% ZrB_2
Al+5.0% ZrB_2
Al+7.5% ZrB_2
Al+10.0% ZrB_2
Al+10.0% VB_2
ref
Al 00-004-0787
ZrB_2 00-034-0423
VB_2 00-038-1463
Al_3Zr 00-048-1385)

(i)

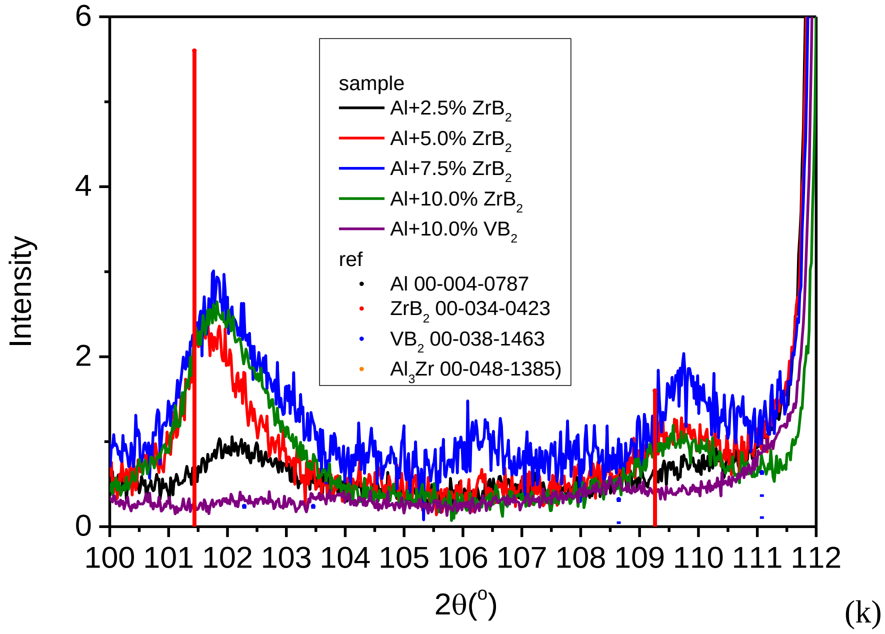

Figure 4.11. XRD analysis of samples A, B, C, D - for the whole range of values of the angle 2θ (a), for ssαAl (j) or for the compounds ZrAl$_3$ (b, h, i) and ZrB$_2$ (b, d ÷ k)

For the determinations performed, the databases of the D8 ADVANCE diffractometer were used, namely sheet 00-048-1385 for Al$_3$Zr and sheet 00-04-0423 for ZrB$_2$, in which are specified, for pure substances, the crystallographic systems in which it crystallizes, the parameters elementary cell, interatomic distances, densities, molar masses, etc.

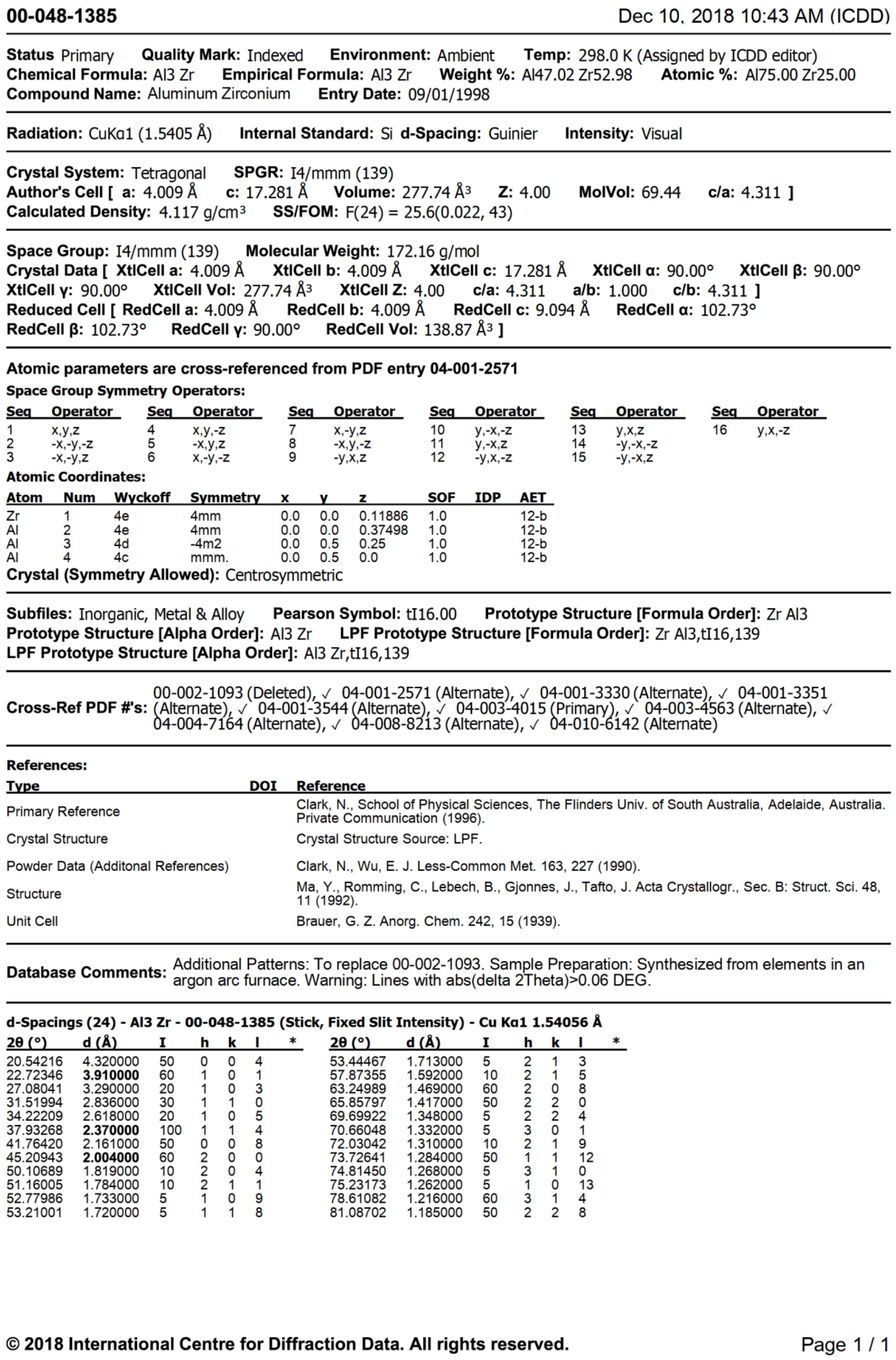

00-048-1385 Dec 10, 2018 10:43 AM (ICDD)

Status Primary **Quality Mark:** Indexed **Environment:** Ambient **Temp:** 298.0 K (Assigned by ICDD editor)
Chemical Formula: Al3 Zr **Empirical Formula:** Al3 Zr **Weight %:** Al47.02 Zr52.98 **Atomic %:** Al75.00 Zr25.00
Compound Name: Aluminum Zirconium **Entry Date:** 09/01/1998

Radiation: CuKα1 (1.5405 Å) **Internal Standard:** Si **d-Spacing:** Guinier **Intensity:** Visual

Crystal System: Tetragonal **SPGR:** I4/mmm (139)
Author's Cell [a: 4.009 Å **c:** 17.281 Å **Volume:** 277.74 Å^3 **Z:** 4.00 **MolVol:** 69.44 **c/a:** 4.311 **]**
Calculated Density: 4.117 g/cm^3 **SS/FOM:** F(24) = 25.6(0.022, 43)

Space Group: I4/mmm (139) **Molecular Weight:** 172.16 g/mol
Crystal Data [XtlCell a: 4.009 Å **XtlCell b:** 4.009 Å **XtlCell c:** 17.281 Å **XtlCell α:** 90.00° **XtlCell β:** 90.00° **XtlCell γ:** 90.00° **XtlCell Vol:** 277.74 Å^3 **XtlCell Z:** 4.00 **c/a:** 4.311 **a/b:** 1.000 **c/b:** 4.311 **]**
Reduced Cell [RedCell a: 4.009 Å **RedCell b:** 4.009 Å **RedCell c:** 9.094 Å **RedCell α:** 102.73° **RedCell β:** 102.73° **RedCell γ:** 90.00° **RedCell Vol:** 138.87 Å^3 **]**

Atomic parameters are cross-referenced from PDF entry 04-001-2571

Space Group Symmetry Operators:

Seq	Operator	Seq	Operator	Seq	Operator	Seq	Operator	Seq	Operator	Seq	Operator
1	x,y,z	4	x,y,-z	7	x,-y,z	10	y,-x,-z	13	y,x,z	16	y,x,-z
2	-x,-y,-z	5	-x,y,z	8	-x,y,-z	11	y,-x,z	14	-y,-x,-z		
3	-x,-y,z	6	x,-y,-z	9	-y,x,z	12	-y,x,-z	15	-y,-x,z		

Atomic Coordinates:

Atom	Num	Wyckoff	Symmetry	x	y	z	SOF	IDP	AET
Zr	1	4e	4mm	0.0	0.0	0.11886	1.0		12-b
Al	2	4e	4mm	0.0	0.0	0.37498	1.0		12-b
Al	3	4d	-4m2	0.0	0.5	0.25	1.0		12-b
Al	4	4c	mmm.	0.0	0.5	0.0	1.0		12-b

Crystal (Symmetry Allowed): Centrosymmetric

Subfiles: Inorganic, Metal & Alloy **Pearson Symbol:** tI16.00 **Prototype Structure [Formula Order]:** Zr Al3
Prototype Structure [Alpha Order]: Al3 Zr **LPF Prototype Structure [Formula Order]:** Zr Al3,tI16,139
LPF Prototype Structure [Alpha Order]: Al3 Zr,tI16,139

Cross-Ref PDF #'s: 00-002-1093 (Deleted), ✓ 04-001-2571 (Alternate), ✓ 04-001-3330 (Alternate), ✓ 04-001-3351 (Alternate), ✓ 04-001-3544 (Alternate), ✓ 04-003-4015 (Primary), ✓ 04-003-4563 (Alternate), ✓ 04-004-7164 (Alternate), ✓ 04-008-8213 (Alternate), ✓ 04-010-6142 (Alternate)

References:

Type	DOI	Reference
Primary Reference		Clark, N., School of Physical Sciences, The Flinders Univ. of South Australia, Adelaide, Australia. Private Communication (1996).
Crystal Structure		Crystal Structure Source: LPF.
Powder Data (Additonal References)		Clark, N., Wu, E. J. Less-Common Met. 163, 227 (1990).
Structure		Ma, Y., Romming, C., Lebech, B., Gjonnes, J., Tafto, J. Acta Crystallogr., Sec. B: Struct. Sci. 48, 11 (1992).
Unit Cell		Brauer, G. Z. Anorg. Chem. 242, 15 (1939).

Database Comments: Additional Patterns: To replace 00-002-1093. Sample Preparation: Synthesized from elements in an argon arc furnace. Warning: Lines with abs(delta 2Theta)>0.06 DEG.

d-Spacings (24) - Al3 Zr - 00-048-1385 (Stick, Fixed Slit Intensity) - Cu Kα1 1.54056 Å

2θ (°)	d (Å)	I	h	k	l	*
20.54216	4.320000	50	0	0	4	
22.72346	**3.910000**	60	1	0	1	
27.08041	3.290000	20	1	0	3	
31.51994	2.836000	30	1	1	0	
34.22209	2.618000	20	1	0	5	
37.93268	**2.370000**	100	1	1	4	
41.76420	2.161000	50	0	0	8	
45.20943	**2.004000**	60	2	0	0	
50.10689	1.819000	10	2	0	4	
51.16005	1.784000	10	2	1	1	
52.77986	1.733000	5	1	0	9	
53.21001	1.720000	5	1	1	8	
53.44467	1.713000	5	2	1	3	
57.87355	1.592000	10	2	1	5	
63.24989	1.469000	60	2	0	8	
65.85797	1.417000	50	2	2	0	
69.69922	1.348000	5	2	2	4	
70.66048	1.332000	5	3	0	1	
72.03042	1.310000	10	2	1	9	
73.72641	1.284000	50	1	1	12	
74.81450	1.268000	5	3	1	0	
75.23173	1.262000	5	1	0	13	
78.61082	1.216000	60	3	1	4	
81.08702	1.185000	50	2	2	8	

Page 1 / 1

Figure 4.12. Sheet 00-048-1385 for Al$_3$Zr

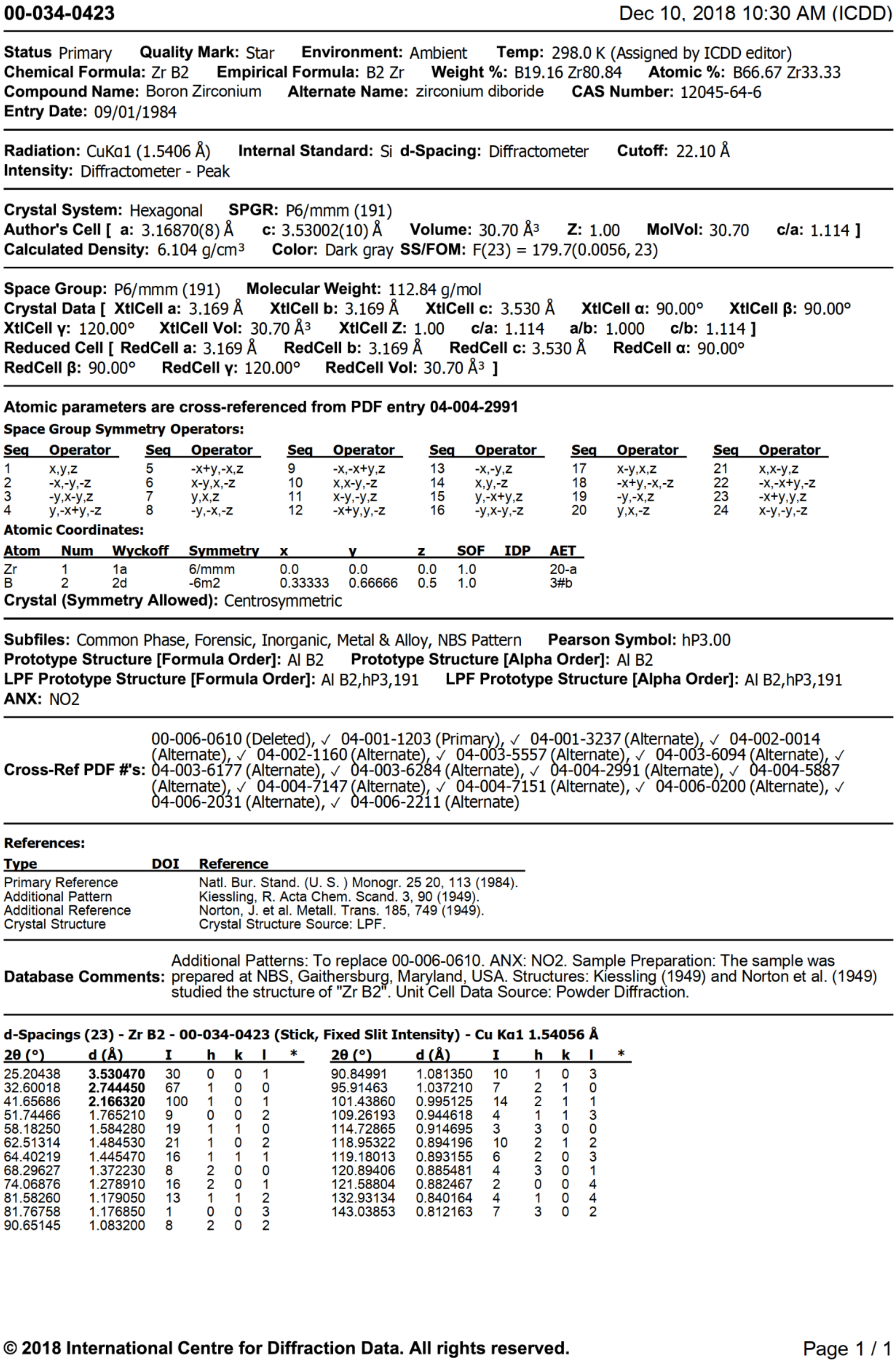

00-034-0423 Dec 10, 2018 10:30 AM (ICDD)

Status Primary **Quality Mark:** Star **Environment:** Ambient **Temp:** 298.0 K (Assigned by ICDD editor)
Chemical Formula: Zr B2 **Empirical Formula:** B2 Zr **Weight %:** B19.16 Zr80.84 **Atomic %:** B66.67 Zr33.33
Compound Name: Boron Zirconium **Alternate Name:** zirconium diboride **CAS Number:** 12045-64-6
Entry Date: 09/01/1984

Radiation: CuKα1 (1.5406 Å) **Internal Standard:** Si **d-Spacing:** Diffractometer **Cutoff:** 22.10 Å
Intensity: Diffractometer - Peak

Crystal System: Hexagonal **SPGR:** P6/mmm (191)
Author's Cell [a: 3.16870(8) Å **c:** 3.53002(10) Å **Volume:** 30.70 Å³ **Z:** 1.00 **MolVol:** 30.70 **c/a:** 1.114 **]**
Calculated Density: 6.104 g/cm³ **Color:** Dark gray **SS/FOM:** F(23) = 179.7(0.0056, 23)

Space Group: P6/mmm (191) **Molecular Weight:** 112.84 g/mol
Crystal Data [XtlCell a: 3.169 Å **XtlCell b:** 3.169 Å **XtlCell c:** 3.530 Å **XtlCell α:** 90.00° **XtlCell β:** 90.00°
XtlCell γ: 120.00° **XtlCell Vol:** 30.70 Å³ **XtlCell Z:** 1.00 **c/a:** 1.114 **a/b:** 1.000 **c/b:** 1.114 **]**
Reduced Cell [RedCell a: 3.169 Å **RedCell b:** 3.169 Å **RedCell c:** 3.530 Å **RedCell α:** 90.00°
RedCell β: 90.00° **RedCell γ:** 120.00° **RedCell Vol:** 30.70 Å³ **]**

Atomic parameters are cross-referenced from PDF entry 04-004-2991

Space Group Symmetry Operators:

Seq	Operator
1	x,y,z
2	-x,-y,-z
3	-y,x-y,z
4	y,-x+y,-z
5	-x+y,-x,z
6	x-y,x,-z
7	y,x,z
8	-y,-x,-z
9	-x,-x+y,z
10	x,x-y,-z
11	x-y,-y,z
12	-x+y,y,-z
13	-x,-y,z
14	x,y,-z
15	y,-x+y,z
16	-y,x-y,-z
17	x-y,x,z
18	-x+y,-x,-z
19	-y,-x,z
20	y,x,-z
21	x,x-y,z
22	-x,-x+y,-z
23	-x+y,y,z
24	x-y,-y,-z

Atomic Coordinates:

Atom	Num	Wyckoff	Symmetry	x	y	z	SOF	IDP	AET
Zr	1	1a	6/mmm	0.0	0.0	0.0	1.0		20-a
B	2	2d	-6m2	0.33333	0.66666	0.5	1.0		3#b

Crystal (Symmetry Allowed): Centrosymmetric

Subfiles: Common Phase, Forensic, Inorganic, Metal & Alloy, NBS Pattern **Pearson Symbol:** hP3.00
Prototype Structure [Formula Order]: Al B2 **Prototype Structure [Alpha Order]:** Al B2
LPF Prototype Structure [Formula Order]: Al B2,hP3,191 **LPF Prototype Structure [Alpha Order]:** Al B2,hP3,191
ANX: NO2

Cross-Ref PDF #'s: 00-006-0610 (Deleted), ✓ 04-001-1203 (Primary), ✓ 04-001-3237 (Alternate), ✓ 04-002-0014 (Alternate), ✓ 04-002-1160 (Alternate), ✓ 04-003-5557 (Alternate), ✓ 04-003-6094 (Alternate), ✓ 04-003-6177 (Alternate), ✓ 04-003-6284 (Alternate), ✓ 04-004-2991 (Alternate), ✓ 04-004-5887 (Alternate), ✓ 04-004-7147 (Alternate), ✓ 04-004-7151 (Alternate), ✓ 04-006-0200 (Alternate), ✓ 04-006-2031 (Alternate), ✓ 04-006-2211 (Alternate)

References:

Type	DOI	Reference
Primary Reference		Natl. Bur. Stand. (U. S.) Monogr. 25 20, 113 (1984).
Additional Pattern		Kiessling, R. Acta Chem. Scand. 3, 90 (1949).
Additional Reference		Norton, J. et al. Metall. Trans. 185, 749 (1949).
Crystal Structure		Crystal Structure Source: LPF.

Database Comments: Additional Patterns: To replace 00-006-0610. ANX: NO2. Sample Preparation: The sample was prepared at NBS, Gaithersburg, Maryland, USA. Structures: Kiessling (1949) and Norton et al. (1949) studied the structure of "Zr B2". Unit Cell Data Source: Powder Diffraction.

d-Spacings (23) - Zr B2 - 00-034-0423 (Stick, Fixed Slit Intensity) - Cu Kα1 1.54056 Å

2θ (°)	d (Å)	I	h	k	l	*
25.20438	**3.530470**	30	0	0	1	
32.60018	**2.744450**	67	1	0	0	
41.65686	**2.166320**	100	1	0	1	
51.74466	1.765210	9	0	0	2	
58.18250	1.584280	19	1	1	0	
62.51314	1.484530	21	1	0	2	
64.40219	1.445470	16	1	1	1	
68.29627	1.372230	8	2	0	0	
74.06876	1.278910	16	2	0	1	
81.58260	1.179050	13	1	1	2	
81.76758	1.176850	1	0	0	3	
90.65145	1.083200	8	2	0	2	
90.84991	1.081350	10	1	0	3	
95.91463	1.037210	7	2	1	0	
101.43860	0.995125	14	2	1	1	
109.26193	0.944618	4	1	1	3	
114.72865	0.914695	3	3	0	0	
118.95322	0.894196	10	2	1	2	
119.18013	0.893155	6	2	0	3	
120.89406	0.885481	4	3	0	1	
121.58804	0.882467	2	0	0	4	
132.93134	0.840164	4	1	0	4	
143.03853	0.812163	7	3	0	2	

Page 1 / 1

Figure 4.13. Sheet 00-034-0423 for ZrB_2

Extraction of ZrB_2 particles from the composite materials was performed by dissolving in 35% HCl solution followed by filtration and drying.

SEM analysis of ZrB_2 powders was performed with the SEM plant (VEGA II LMU). The results are given in Figure 4.14.

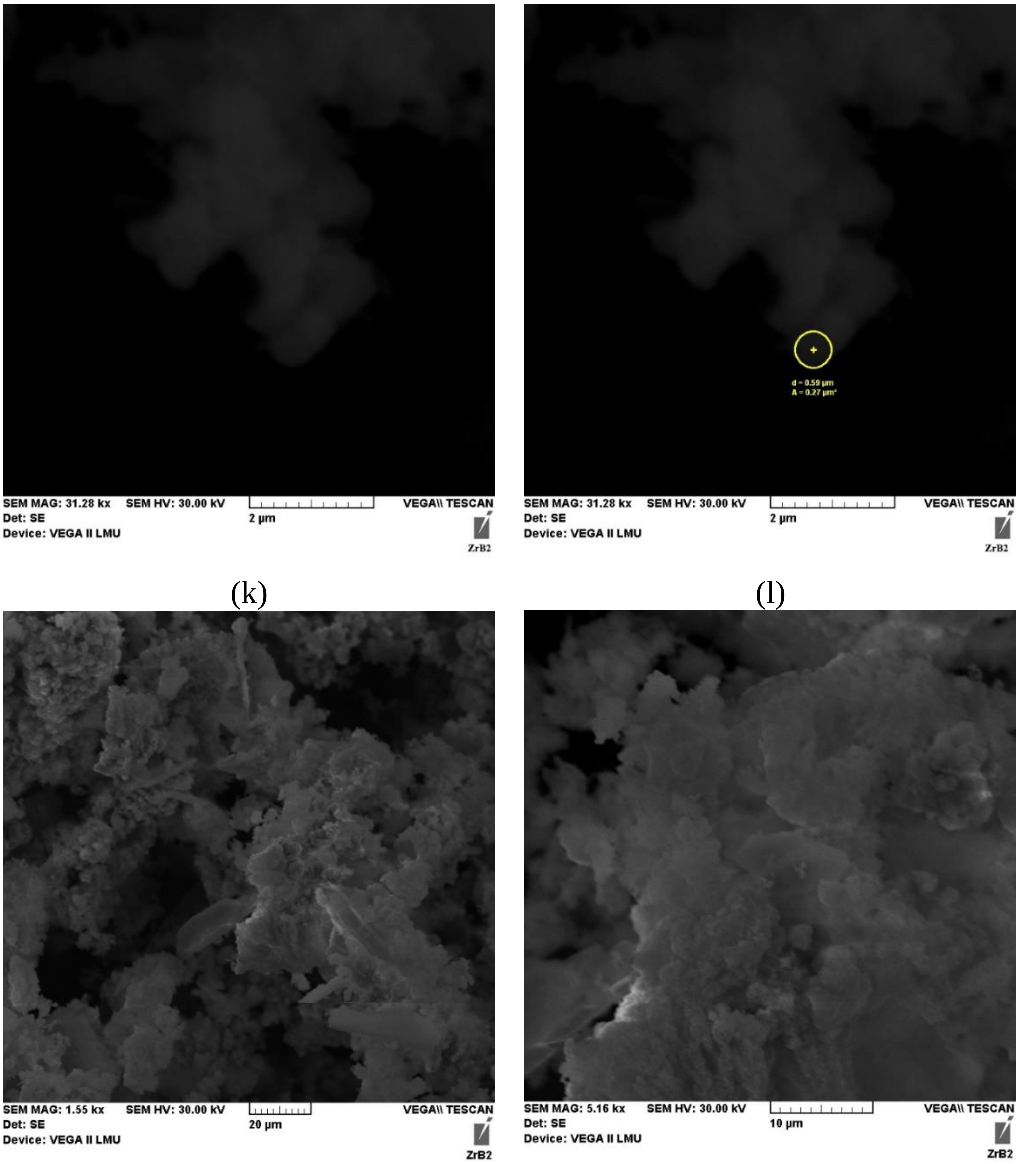

(k) (l)

(m) (n)

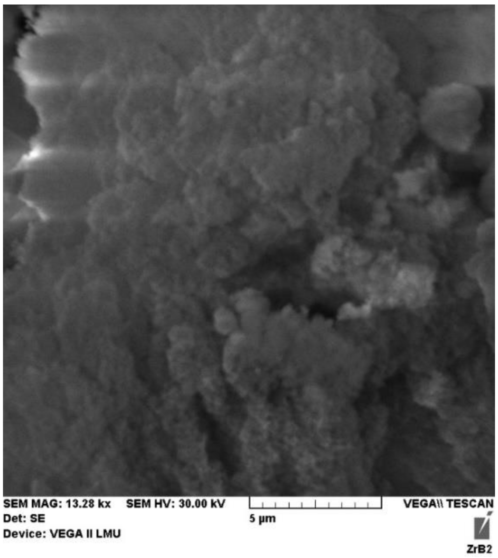

(o)

Figure 4.14. SEM analysis of ZrB_2 powders extracted from composites

ZrB_2 powders extracted from the samples of cast composites with dimensions between 5µm and 20µm were performed HRTEM analysis of the extracted powders (Figure 4.15).

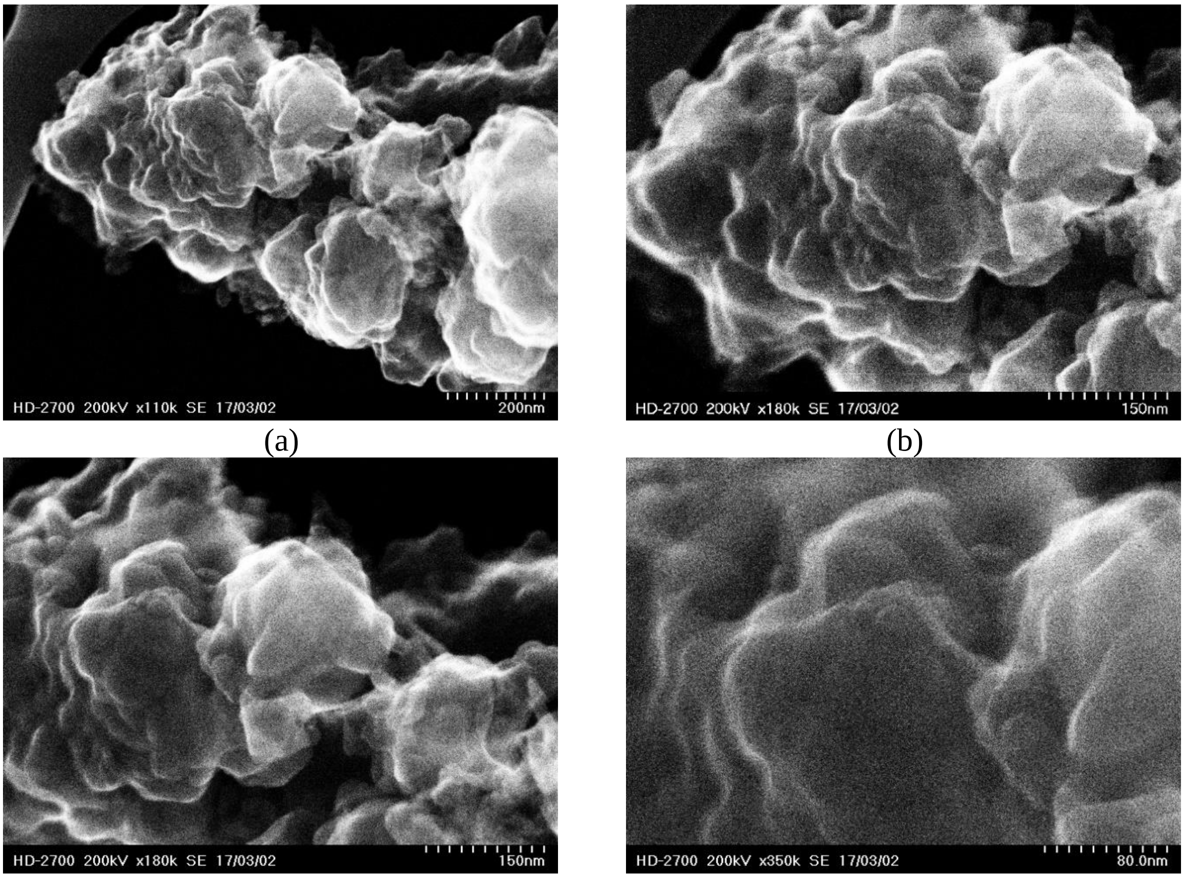

(a) (b)

(c) (d)

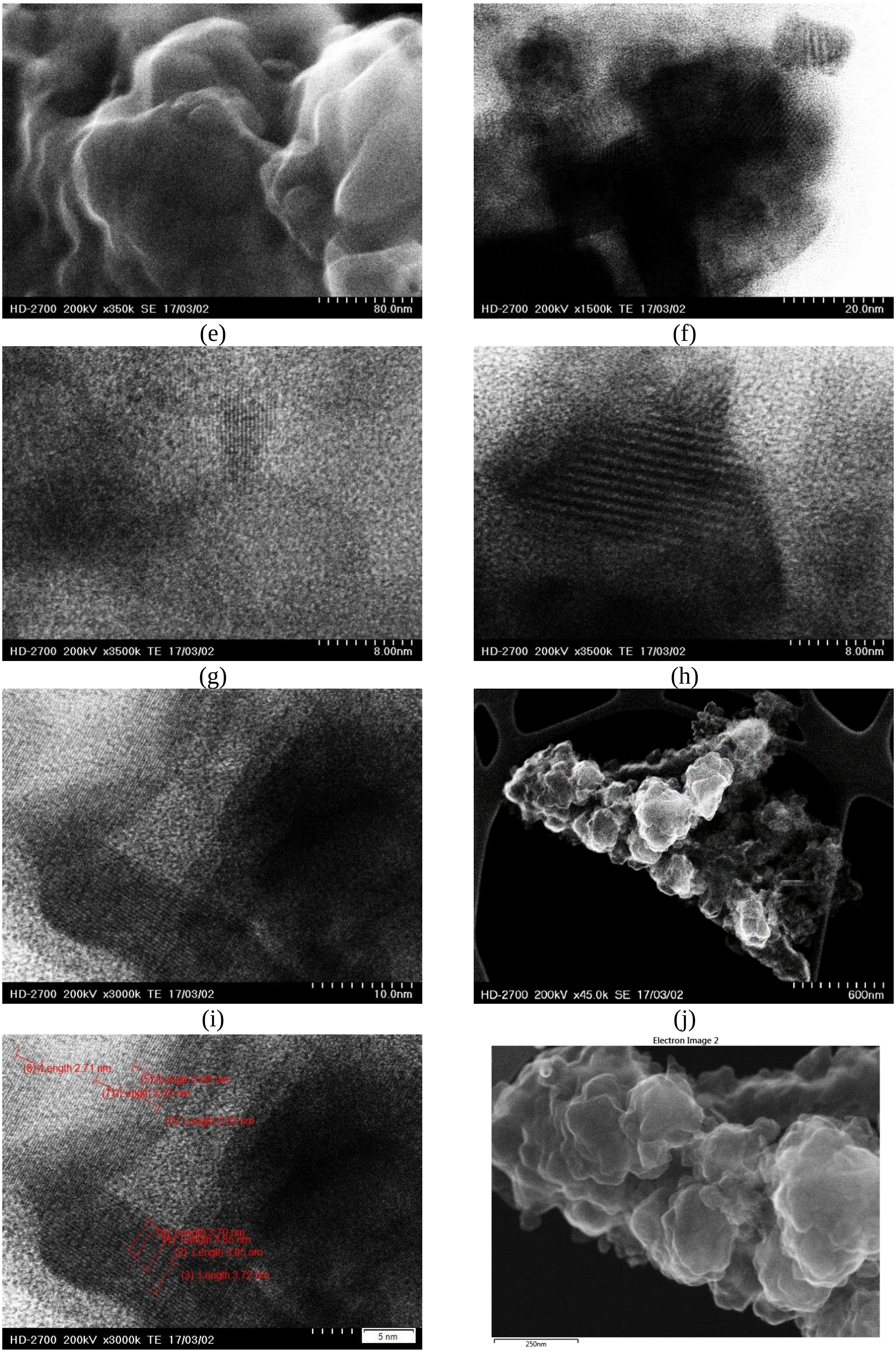

(e) (f)

(g) (h)

(i) (j)

(k) (l)

Figure 4.15. HRTEM images of ZrB_2 powders extracted from processed composite materials

CHAPTER 5. Physio-mechanical properties of AA6063 / ZrB_2 composites

The mechanical properties followed and determined for the elaborated composites were: hardness, mechanical resistance to breakage, tensile, mechanical resistance to compression. Important properties of the reinforcement elements obtained in situ are presented in Table 5.1.

Table 5.1. Physical properties of zirconium diboride (ZrB_2) [81]

IUPAC Name	Theoretical chemical formula, [CASRN]	Crystallographic system, network parameters. Pearson symbol, space group, the type of structure, Z	Thermal conductivity ($k.Wm^{-1}K^{-1}$)	Specific thermal capacity (c_p.J kg^{-1} K^{-1})	Coefficient of linear thermal expansion (α, 10^{-6} K^{-1})
Zirconium diboride	ZrB_2 [12045-64-6] 112.846	Hexagonal *a* = 0,3169 nm c = 0,3530 nm *hP*3, *P6/mmm*, AlB_2 type (*Z* = 1)	57,9	392,54	5,5-8,3

5.1. Hardness

The hardness was determined using a microdurimeter produced by Leco M-400-G, year of manufacture 2004.

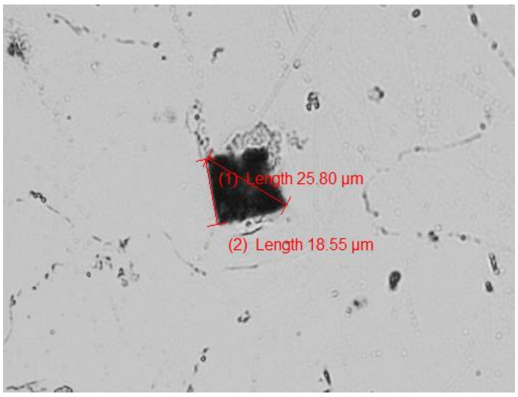

Sample A x200

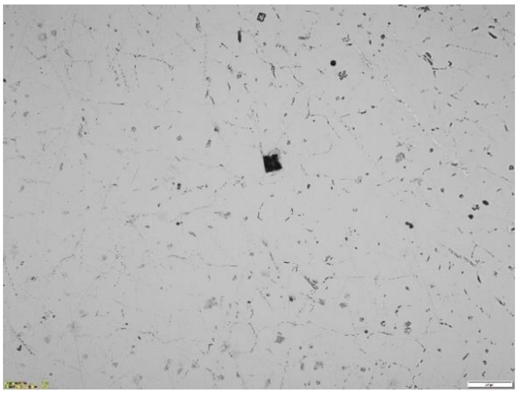

Sample A x200

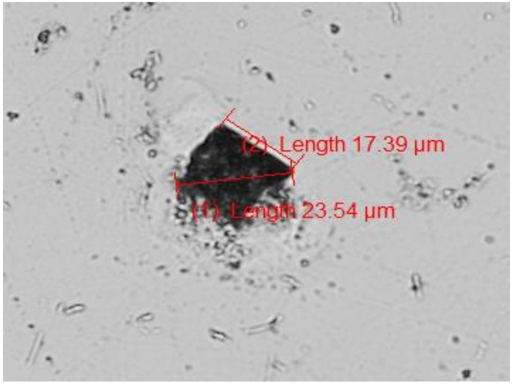

Sample B x200

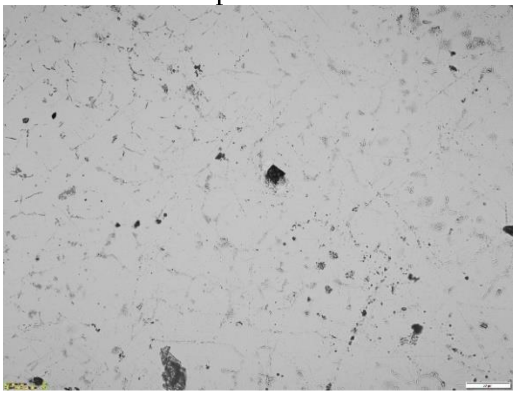

Sample B x200

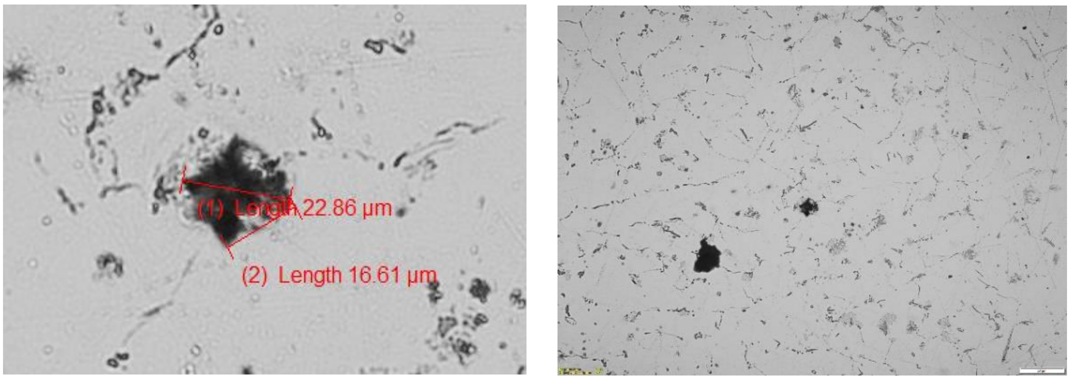

Sample C x200 Sample C x200

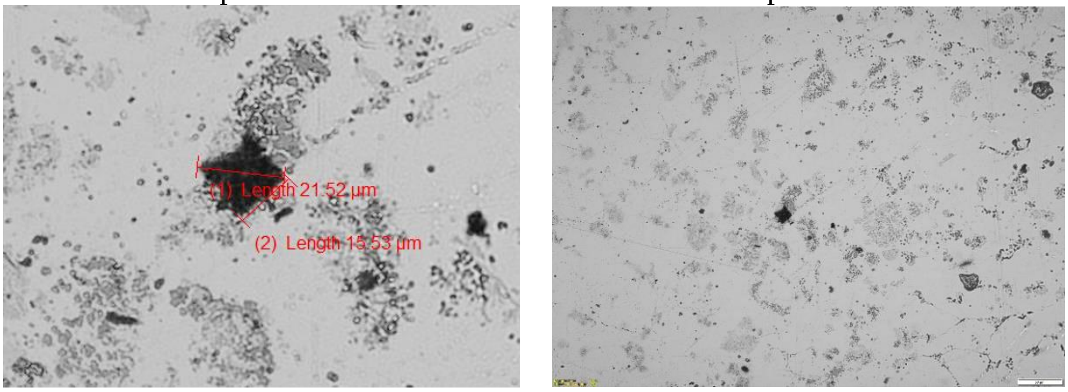

Sample D x200 Sample D x200

Figure 5.1. Determination of the size of the cavities left after the tests for the determination of Vickers microhardness by measurement using optical microscopy

5.2. Tensile strength

Figure 5.2. Samples used to determine tensile and elongation strengths

Data for tensile and elongation strength were taken from the results obtained using the Instron Universal Testing Machine 8872 at room temperature using cylindrical samples 15 mm long and 5 mm in diameter. On average, three samples were used for each test.

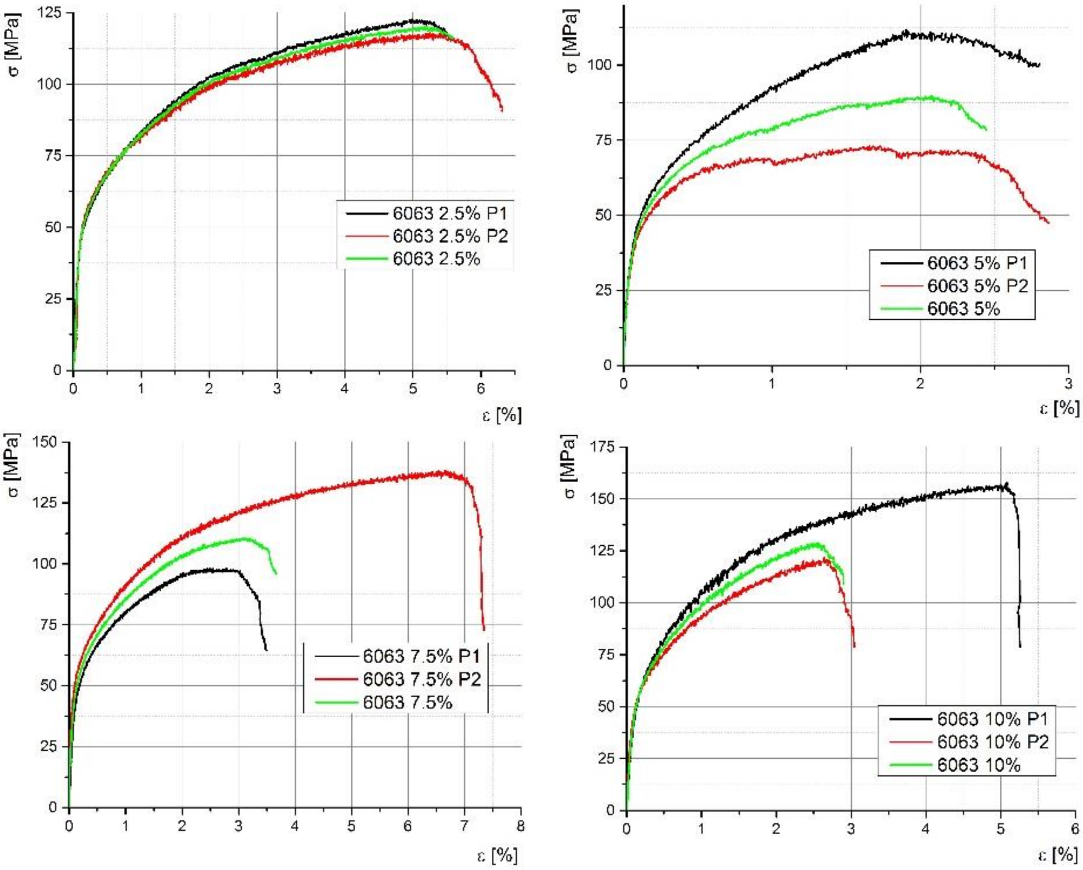

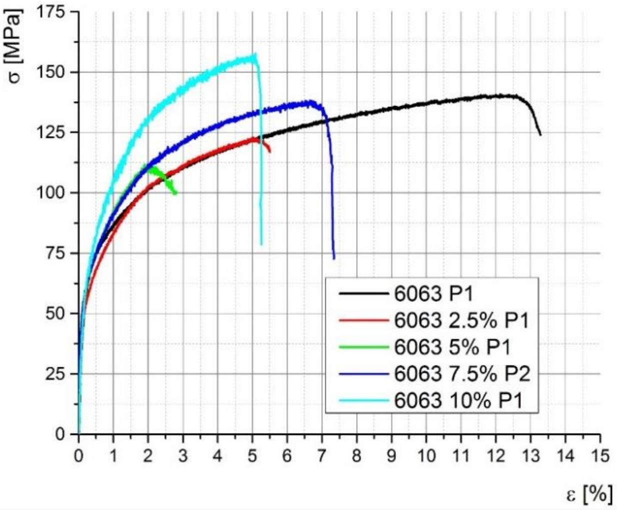

Figure 5.3. Tensile test results for manufactured composite materials

5.3. Compression strength

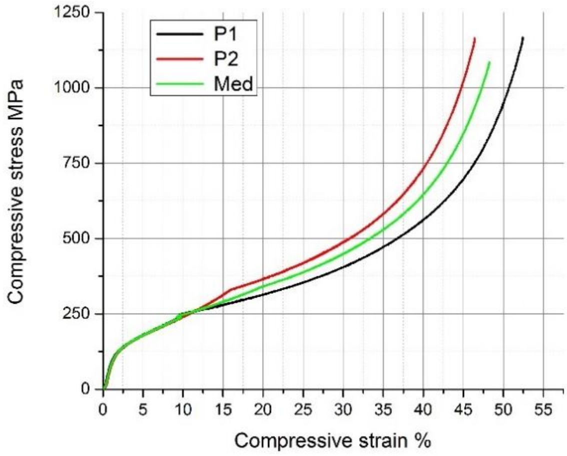

Compression Sample A (AA6063/2,5% ZrB_2)

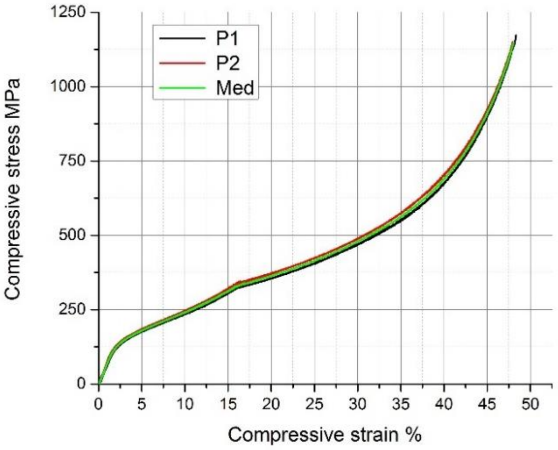

Compression Sample B (AA6063/5% ZrB_2)

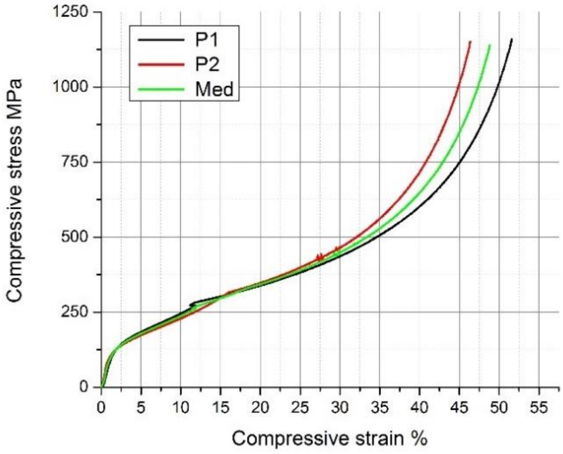

Compression Sample C (AA6063/7,5% ZrB_2)

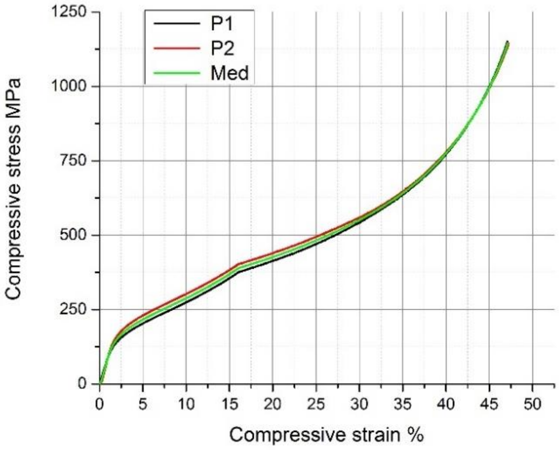

Compression Sample D (AA6063/10% ZrB_2)

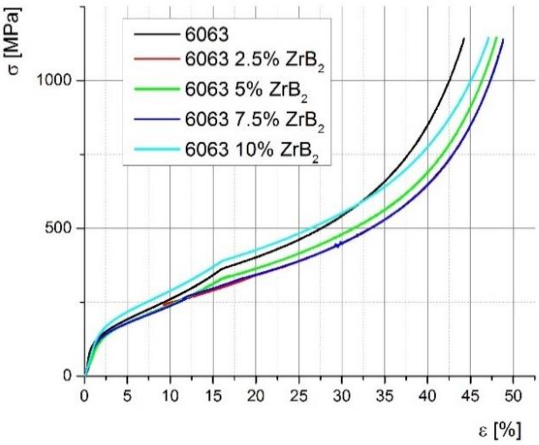

Figure 5.4. Compression test results for manufactured composites

5.4. Study of fractography of samples of cast composites

The in-depth study of the fracture surfaces was performed by SEM analysis using the HITACHI HD-2300 microscope (scanning transmission electron microscope).

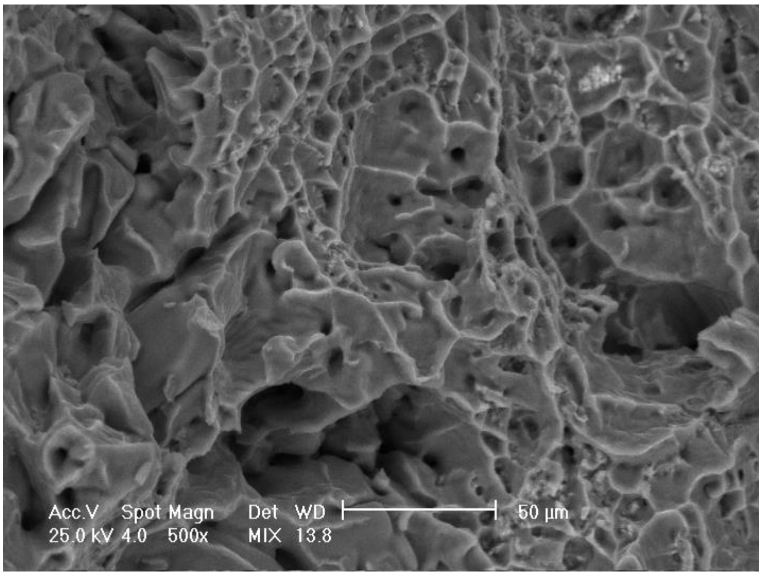

Figure 5.5. SEM in fracture at composite AA6063/2,5% ZrB_2 (Sample A)

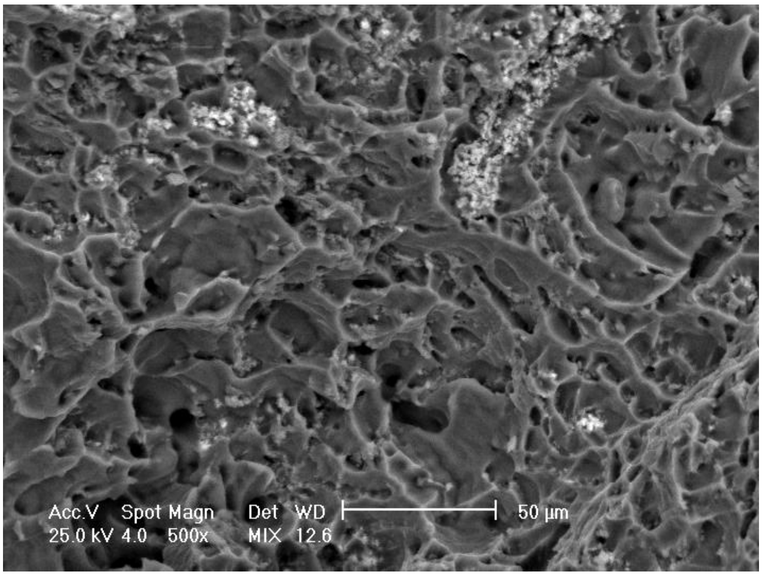

Figure 5.6. SEM in fracture at composite AA6063/5% ZrB_2 (Sample B)

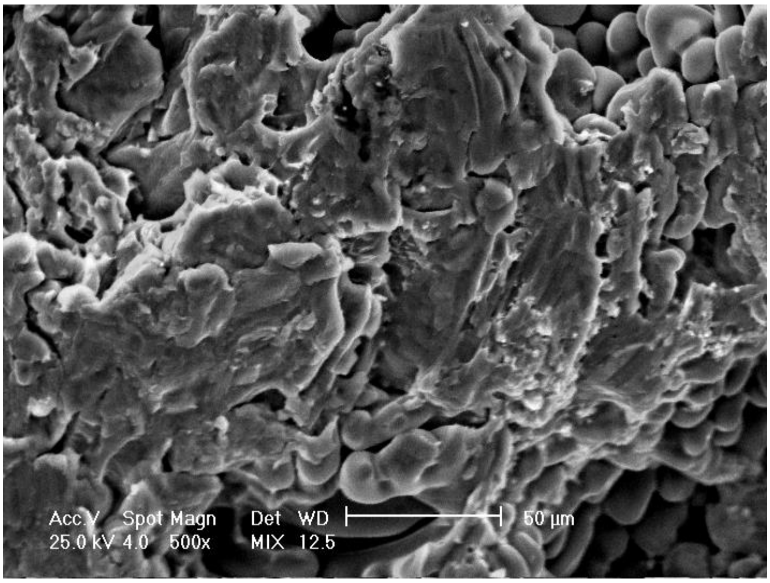

Figure 5.7. SEM in fracture at composite AA6063/7,5% ZrB_2 (Sample C)

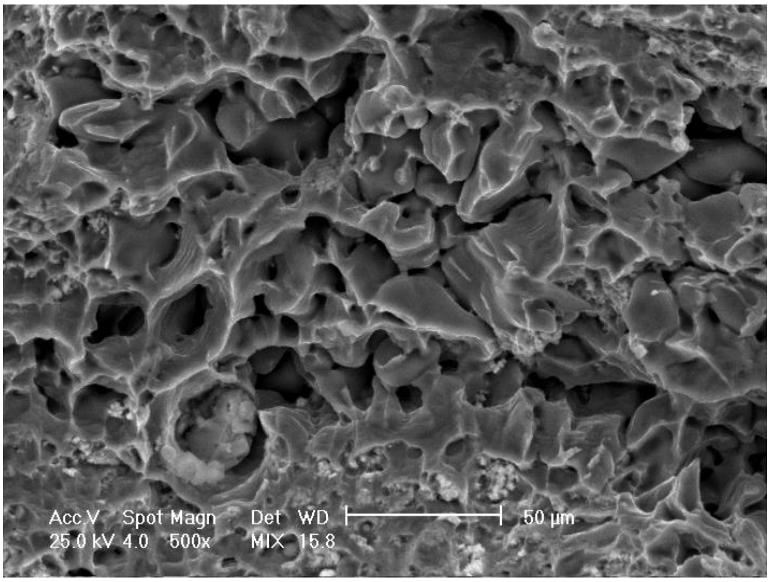

Figure 5.8. SEM rupture at composite AA6063/10% ZrB_2 (Sample D)

5.5. The coefficient of expansion and diffusivity of the elaborated composites

Any property of a material studied in a temperature range can be considered a thermophysical property. However, traditionally, thermal expansion, thermal conductivity and thermal diffusivity are considered to be the most common fundamental thermophysical properties.

A. Thermal expansion

The purpose of this method is to determine the coefficient of linear thermal expansion (CTE) for some materials with coefficients of linear thermal expansion greater than ± 1 micron / ° C, using a dilatometer with high purity sintered alumina components.

Thermal expansion coefficient analysis is a thermal method of tracking the dimensional variability of a sample as a function of temperature and time.

The determination of the thermal expansion coefficient was performed with the help of the thermal dilatometer model Unitherm 1161V (Fig. 5.9).

Figure 5.9. Vertical thermal dilatometer, model Unitherm 1161V

The temperature values between which this test is performed are in the range of 20 - 600°C. This method is not used for materials with coefficients of thermal expansion less than 1x10-6 / °C; below this value the interferometer or other capacitive measuring techniques are recommended.

The experimental data, respectively the dilatograms, for the four samples, taken from the composite materials with 2.5%, 5.0%, 7.5% and 10.0% ZrB2, respectively, are presented in Fig. 5.10.

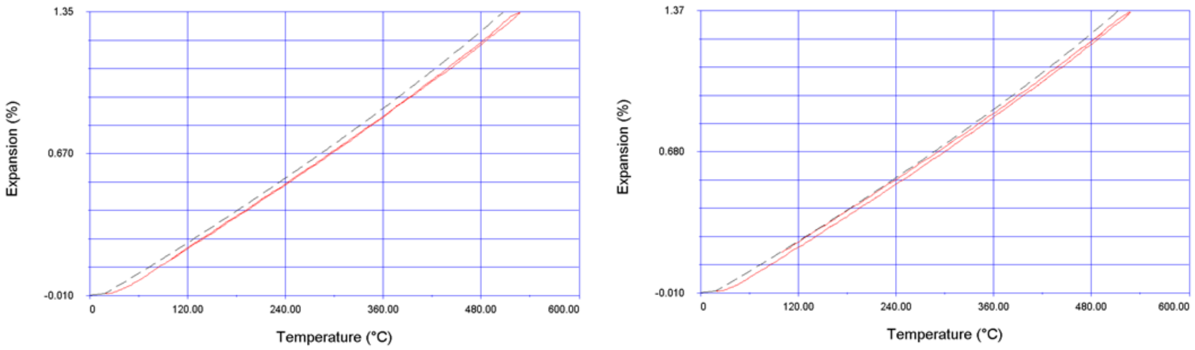

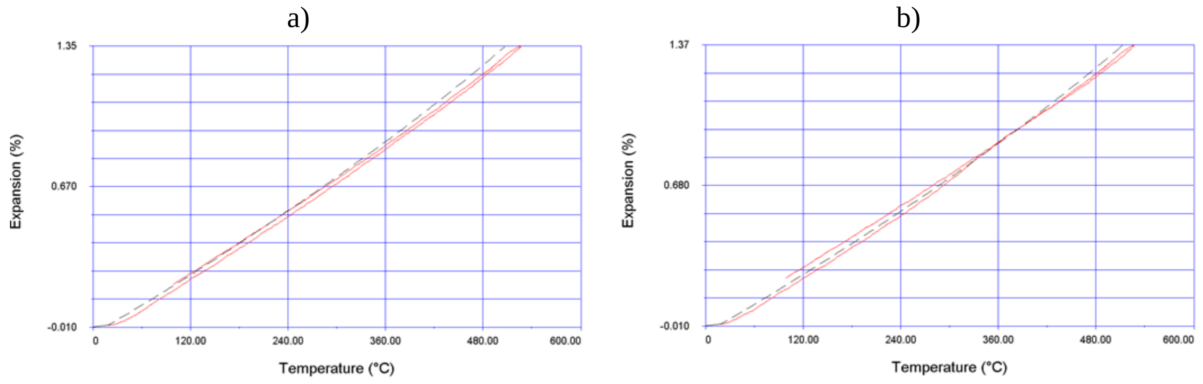

c) d)

Figure 5.10. Dilatograms, for the four samples, taken from composite materials with (a) 2.5%, (b) 5.0%, (c) 7.5% and (d) 10.0% ZrB_2, respectively

In Figure 5.11. the results are presented in numerical and graphical format, respectively, of the percentage coefficient of thermal expansion (E%), of the instantaneous coefficient of thermal expansion (CTE) and respectively of the average coefficient of linear thermal expansion (A-CTE).

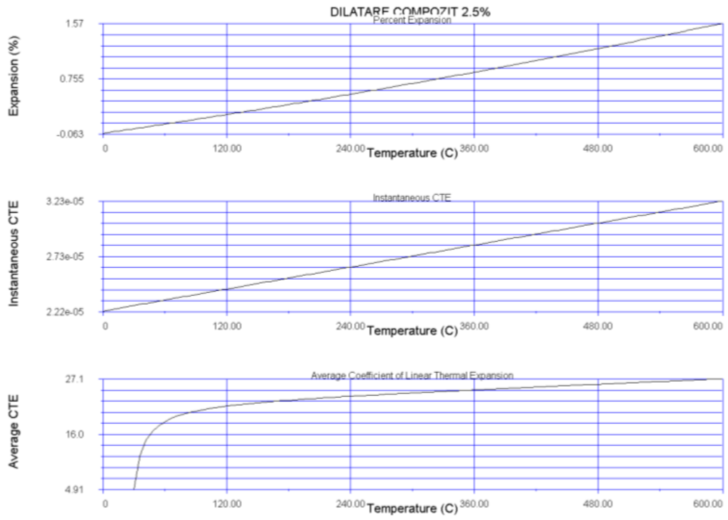

```
Temp.     Expansion  Inst.Alpha    Avg. Alpha
 (C)         (%)     (x10-6/C)     (x10-6/C)

   0      -0.06251     22.220        31.253
 100       0.16809     23.899        21.011
 200       0.41548     25.579        23.082
 300       0.67967     27.258        24.274
 400       0.96065     28.938        25.280
 500       1.25843     30.618        26.217
 600       1.57300     32.297        27.121
 700       1.90437     33.977        28.005
 800       2.25253     35.656        28.879
 900       2.61749     37.336        29.744
1000       2.99925     39.015        30.605
1100       3.39780     40.695        31.461
1200       3.81314     42.374        32.315
1300       4.24528     44.054        33.166
1400       4.69422     45.733        34.016
1500       5.15995     47.413        34.865
1600       5.64247     49.092        35.712
1700       6.14180     50.772        36.558
1800       6.65791     52.451        37.404
1900       7.19082     54.131        38.249
2000       7.74053     55.811        39.094
```

a) 2.5% ZrB_2

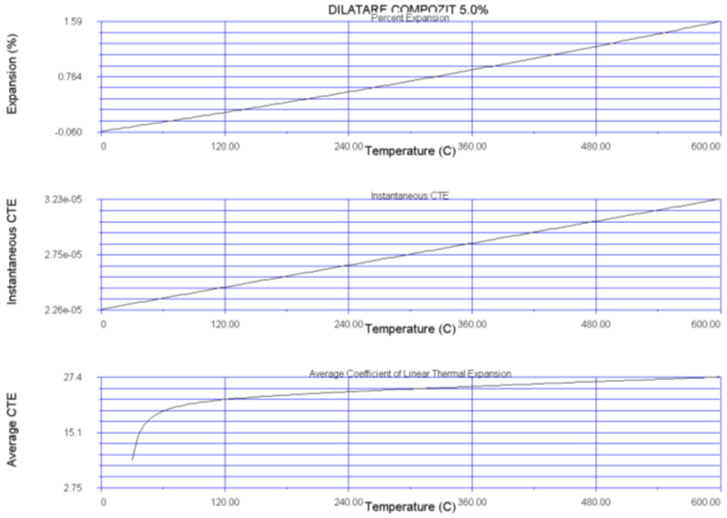

```
Temp.     Expansion  Inst.Alpha    Avg. Alpha
 (C)         (%)     (x10-6/C)     (x10-6/C)

   0      -0.05976     22.628        29.878
 100       0.17457     24.237        21.821
 200       0.42498     25.845        23.610
 300       0.69148     27.454        24.696
 400       0.97406     29.063        25.633
 500       1.27274     30.672        26.515
 600       1.58750     32.281        27.371
 700       1.91835     33.890        28.211
 800       2.26529     35.498        29.042
 900       2.62832     37.107        29.867
1000       3.00744     38.716        30.688
1100       3.40264     40.325        31.506
1200       3.81394     41.934        32.322
1300       4.24132     43.543        33.135
1400       4.68479     45.151        33.948
1500       5.14435     46.760        34.759
1600       5.61999     48.369        35.570
1700       6.11173     49.978        36.379
1800       6.61955     51.587        37.188
1900       7.14346     53.196        37.997
2000       7.68346     54.804        38.805
```

b) 5.0% ZrB_2

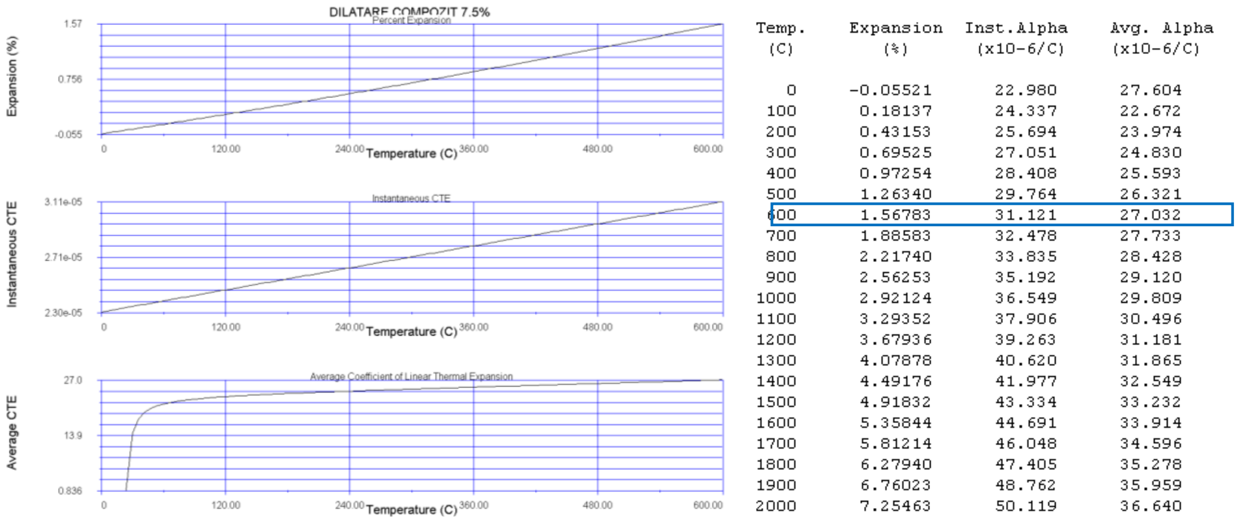

```
Temp.    Expansion   Inst.Alpha    Avg. Alpha
 (C)        (%)      (x10-6/C)     (x10-6/C)

   0     -0.05521      22.980       27.604
 100      0.18137      24.337       22.672
 200      0.43153      25.694       23.974
 300      0.69525      27.051       24.830
 400      0.97254      28.408       25.593
 500      1.26340      29.764       26.321
 600      1.56783      31.121       27.032
 700      1.88583      32.478       27.733
 800      2.21740      33.835       28.428
 900      2.56253      35.192       29.120
1000      2.92124      36.549       29.809
1100      3.29352      37.906       30.496
1200      3.67936      39.263       31.181
1300      4.07878      40.620       31.865
1400      4.49176      41.977       32.549
1500      4.91832      43.334       33.232
1600      5.35844      44.691       33.914
1700      5.81214      46.048       34.596
1800      6.27940      47.405       35.278
1900      6.76023      48.762       35.959
2000      7.25463      50.119       36.640
```

c) *7.5% ZrB_2*

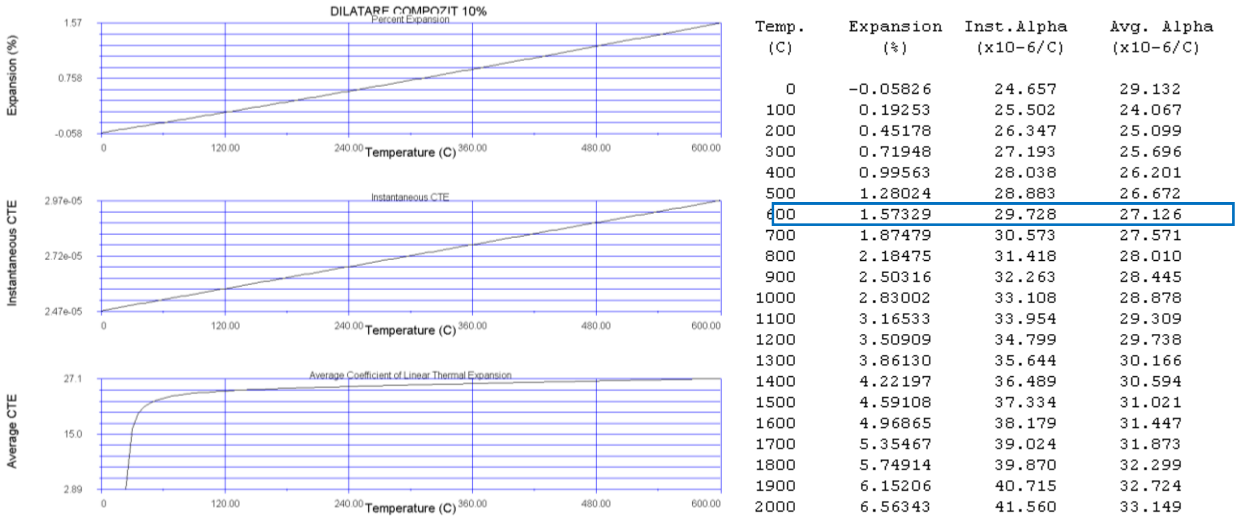

```
Temp.    Expansion   Inst.Alpha    Avg. Alpha
 (C)        (%)      (x10-6/C)     (x10-6/C)

   0     -0.05826      24.657       29.132
 100      0.19253      25.502       24.067
 200      0.45178      26.347       25.099
 300      0.71948      27.193       25.696
 400      0.99563      28.038       26.201
 500      1.28024      28.883       26.672
 600      1.57329      29.728       27.126
 700      1.87479      30.573       27.571
 800      2.18475      31.418       28.010
 900      2.50316      32.263       28.445
1000      2.83002      33.108       28.878
1100      3.16533      33.954       29.309
1200      3.50909      34.799       29.738
1300      3.86130      35.644       30.166
1400      4.22197      36.489       30.594
1500      4.59108      37.334       31.021
1600      4.96865      38.179       31.447
1700      5.35467      39.024       31.873
1800      5.74914      39.870       32.299
1900      6.15206      40.715       32.724
2000      6.56343      41.560       33.149
```

d) *10.0% ZrB_2*

Figure 5.11. The results in graphical and numerical format, respectively, of the percentage coefficient of thermal expansion (E%), of the instantaneous coefficient of thermal expansion (CTE) and of the average coefficient of linear thermal expansion (A-CTE), respectively, for: (a) 2.5%ZrB_2; (b) 5.0%ZrB_2; (c) 7.5%ZrB_2; (d) 10.0%ZrB_2

B) Thermal diffusivity

Thermal diffusivity is one of the most important transient thermal properties of materials. Since thermal diffusivity is a measure of the speed with which heat passes through a material, its importance is indirect but seems linearly related to the speed of things around us.

The experimental diffusivity data, for the four samples, taken from composite materials with 2.5%, 5.0%, 7.5% and 10.0% ZrB_2, respectively, are presented in Tables 5.2, 5.3, 5.4 and 5.5.

Table 5.2 – Thermal diffusivity values for the composite sample with 2.5% ZrB_2

Segment	**Temperatura [ºC]**	**α_{mediu} [cm^2/sec]**	**α_1 [cm^2/sec]**	**α_2 [cm^2/sec]**	**α_3 [cm^2/sec]**	**α_4 [cm^2/sec]**	**α_5 [cm^2/sec]**	**α_6 [cm^2/sec]**
A	**89**	**0,6993**	0,7062	0,6946	0,7113	0,7357	0,5838	0,7643
B	**209**	**0,7671**	0,7629	0,7713	0,7552	0,7773	0,7651	0,7708
C	**329**	**0,7613**	0,7616	0,7626	0,7598	0,7615	0,7603	0,7621
D	**423**	**0,7362**	eroare	eroare	0,7364	eroare	eroare	0,7401

E	**529**	**0,6888**	0,7106	0,7125	0,7242	eroare	0,6609	0,6359

Table 5.3 – Thermal diffusivity values for the composite sample with 5% ZrB_2

Segment	**Temperature [^{o}C]**	**α_{mediu} [cm^2/sec]**	**α_1 [cm^2/sec]**	**α_2 [cm^2/sec]**	**α_3 [cm^2/sec]**	**α_4 [cm^2/sec]**	**α_5 [cm^2/sec]**	**α_6 [cm^2/sec]**
A	**89**	**0,6999**	0,6966	0,7033	0,6965	0,6967	0,7033	0,7032
B	**239**	**0.7725**	0,7698	0,7767	0,7750	0,7712	0,7715	0,7710
C	**369**	**0,6899**	0,6898	0,6899	0,6897	0,6999	0,6900	eroare
D	**427**	**0,6558**	0,6490	0,6558	0,6507	0,6609	0,6558	0,6626
E	**485**	**0,5945**	0,5943	0,5842	0,5945	0,6008	0,5944	0,5990

Table 5.4 – Thermal diffusivity values for the composite sample with 7.5% ZrB_2

Segment	**Temperature [^{o}C]**	**α_{mediu} [cm^2/sec]**	**α_1 [cm^2/sec]**	**α_2 [cm^2/sec]**	**α_3 [cm^2/sec]**	**α_4 [cm^2/sec]**	**α_5 [cm^2/sec]**	**α_6 [cm^2/sec]**
A	**75**	**0,7776**	0,7776	0,7777	0,7778	0,7776	0,7775	0,7778
B	**236**	**0,7509**	0,7446	0,7456	0,7539	0,7549	0,7560	0,7508
C	**388**	**0,7063**	0,7146	0,6981	0,7063	eroare	0,7062	eroare
D	**465**	**0,6550**	0,6649	0,6650	0,6651	0,6650	0,6648	0,6652
E	**531**	**0,5843**	eroare	0,5842	0,5844	0,5843	eroare	eroare

Table 5.5 – Thermal diffusivity values for the composite sample with 10% ZrB_2

Segment	**Temperature [^{o}C]**	**α_{mediu} [cm^2/sec]**	**α_1 [cm^2/sec]**	**α_2 [cm^2/sec]**	**α_3 [cm^2/sec]**	**α_4 [cm^2/sec]**	**α_5 [cm^2/sec]**	**α_6 [cm^2/sec]**
A	**112**	**0,7342**	0,7187	0,7446	eroare	0,7187	0,7446	0,7446
B	**254**	**0.7728**	eroare	0,7725	0,7765	0,7765	0,7693	0,7693
C	**398**	**0,7374**	0,7374	0,7417	0,7291	eroare	0,7374	0,7417
D	**475**	**0,6570**	eroare	eroare	0,6273	0,6867	0,6867	0,6273
E	**530**	**0,6476**	0,6364	0,6365	0,6589	0,6570	0,6484	0,6485

The graphical representation of the thermal diffusivity as a function of temperature, corresponding to the values presented in Tables 5.6, 5.7, 5.8 and 5.9, is shown in Fig. 5.12.

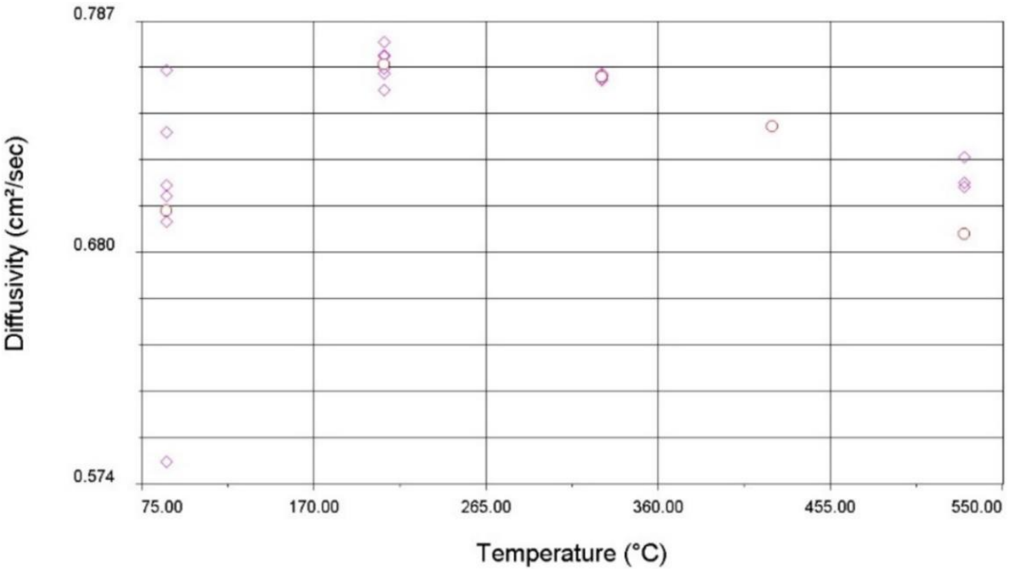

(a) – 2.5%ZrB_2

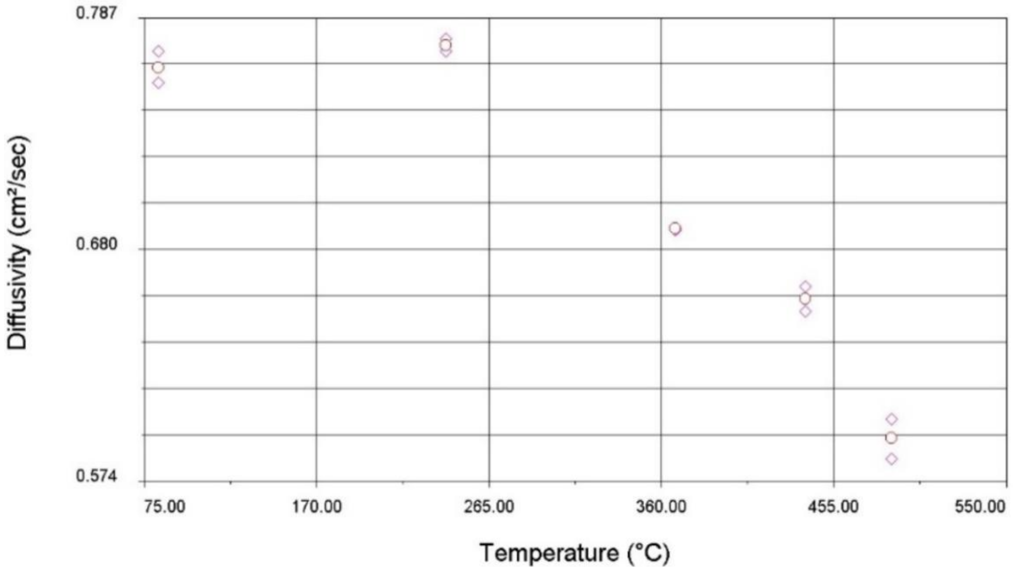

(b) – 5.0%ZrB$_2$

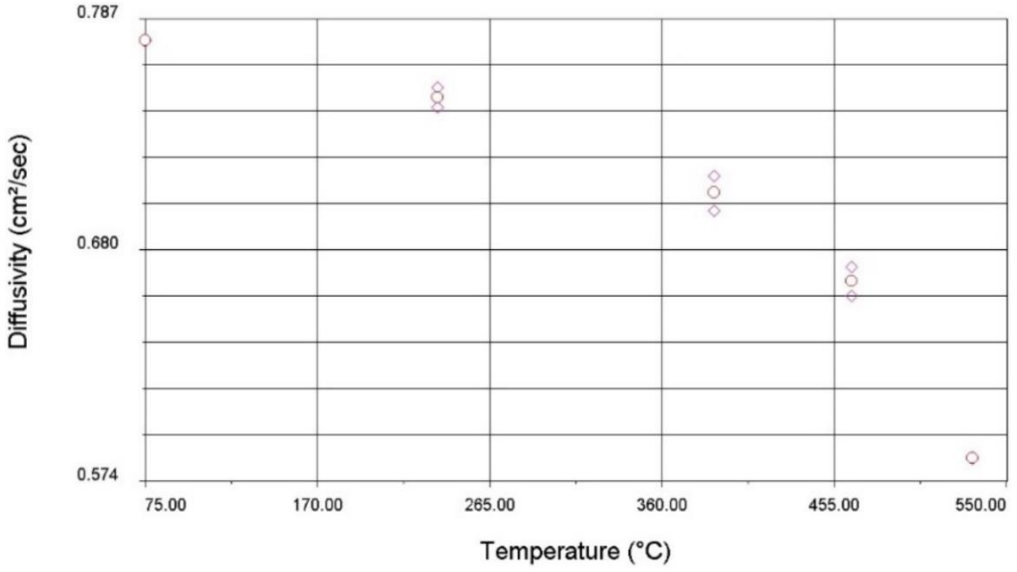

(c) – 7.5%ZrB$_2$

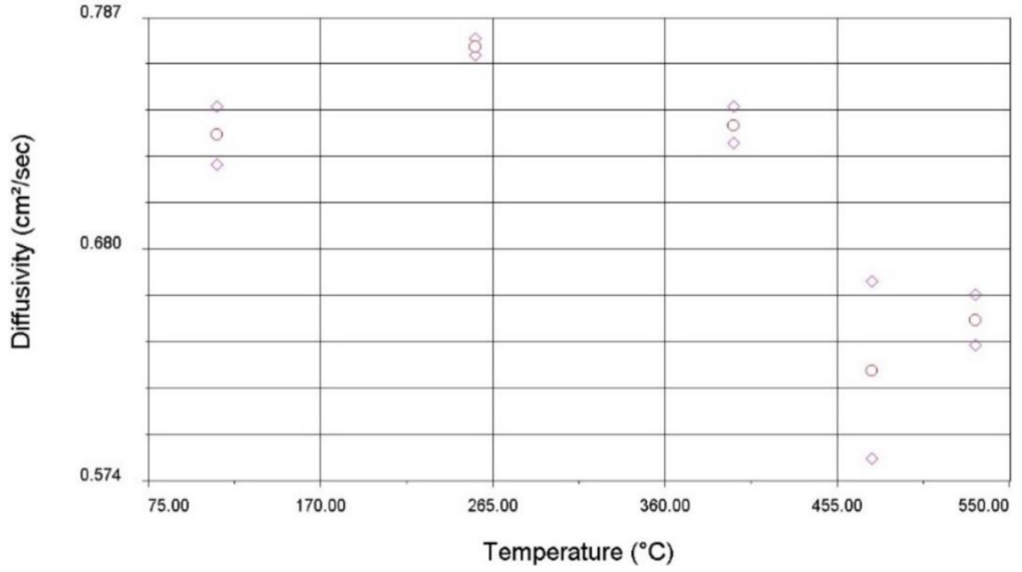

(d) – 10%ZrB$_2$

Figure 5.12 - Graphical representation of thermal diffusivity as a function of temperature, corresponding to the values presented in Tables 5.1 (a), 5.2 (b), 5.3 (c) and 5.4 (d).

In order to verify the correctness of the obtained results, a reference material, respectively a composite graphite (Thermal Graphite-TG) was tested; the tabulated values of the thermal diffusivity, as well as the graphical representation, are presented in Table 5.6, respectively Fig. 5.13.

Table 5.6 - Thermal diffusivity values for the standard composite graphite sample (**Thermal Graphite-TG)**, measured and compared with the values in the Compliance Bulletin

Segment	**Temperature [^{o}C]**	**α_{mediu} [cm^2/sec]**	**α_1 [cm^2/sec]**	**α_2 [cm^2/sec]**	**α_3 [cm^2/sec]**	**α_4 [cm^2/sec]**	**α_5 [cm^2/sec]**	**α_6 [cm^2/sec]**
A	**90**	**0,4300**	0,4277	0,4212	0,4236	0,4558	0,4355	0,4164
TG(etalon)	***100***	***0,4440***						
B	**210**	**0,3272**	0,3283	0,3282	0,3222	0,3306	0,3250	0,3286
TG(etalon)	***200***	***0,3540***						
C	**329**	**0,2600**	0,2664	0,2604	0,2604	0,2600	0,2553	0,2573
TG(etalon)	***300***	***0,2880***						
D	**424**	**0,2256**	0,2321	0,2257	0,2254	0,2251	0,2223	0,2229
TG(etalon)	***400***	***0,2430***						
E	**529**	**0,1973**	0,1980	0,1986	0,1983	0,1979	0,1975	0,1936
TG(etalon)	***500***	***0,212***						

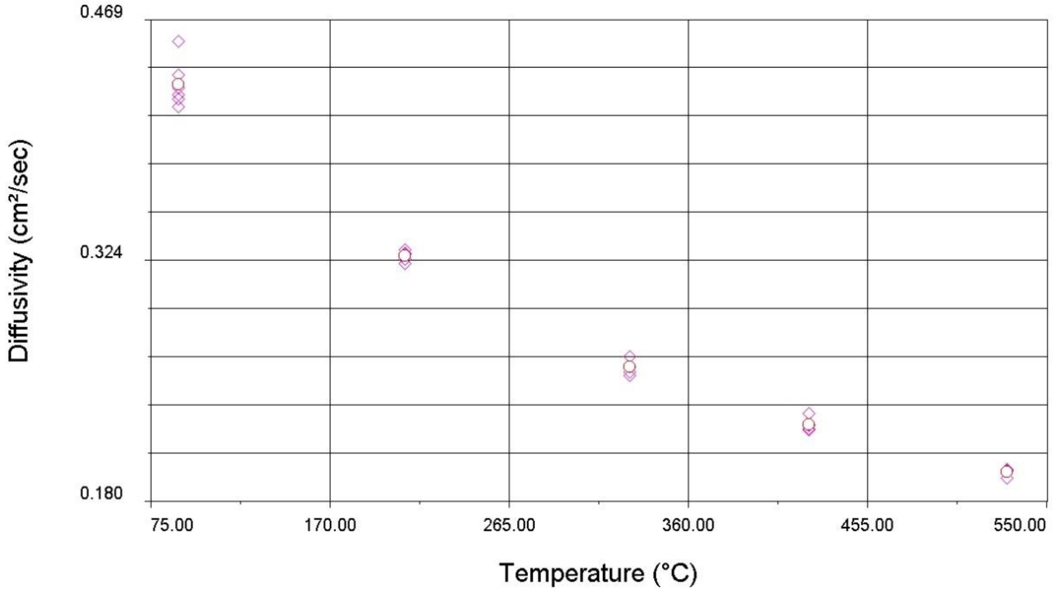

Figure 5.13 - Graphical representation of thermal diffusivity as a function of temperature, corresponding to the values presented in Table 5.5

CHAPTER 6. Summary of the main scientific and technical contributions of the author

Increasing demand for high-density, low-density materials in the aerospace and automotive industries makes aluminium matrix composites (AMCS) a leading candidate for a number of applications.

Thus, a large number of AMCS composites replace conventional aluminium alloys due to the combination of properties such as: high wear resistance, low coefficient of thermal expansion and a high strength / mass ratio. Graphite particles, carbides (SiC), oxides (Al_2O_3), nitrides are mainly used as reinforcement materials.

From different ceramic reinforcement materials, we chose zirconium boride (ZrB_2) because it has high melting temperature, high hardness, high density (2g / cm^3), high coefficient of thermal expansion ($6.88x10^{-6}K^{-1}$), thermal inertia, high electrical conductivity, high chemical inertia.

AMCS composites can be produced in either solid or liquid state. From the two categories of processes, we chose the liquid process. This procedure can be "ex-situ" or "in-situ".

For the production of AA6063 / ZrB_2 composites we chose the in-situ process. While the “ex-situ” process involves mixing the particles in the melt, the “in-situ” process consists of chemical reactions between elements or between elements or compounds to obtain the reinforcing particles directly in the melt.

The merit of the "in-situ" process of forming ZrB_2 in the aluminium alloy melt is that it generates fine ceramic particles of ZrB_2 and Al_3Zr, a very good interfacial bond between the matrix and the particles formed by the reaction between K_2ZrF_6, KBF_4 and Al, and the ZrB_2 particles increase the ductility when finishing the granulation of the cast products.

CHAPTER 7. Conclusions and further research directions

The present work led to the realization of new materials with controllable properties in the radial direction. The following results of the thesis can be considered as original:

- Extensive documentary study on composite materials - their classification according to the basic matrix and the reinforcing elements.
- Documentary study on the structure and properties of composite materials compared to the structure and properties of classical metallic materials.
- The study of the thermodynamics of the phenomena that take place in the system AA6063 - K_2ZrF_6 - KBF_4 - Na_3AlF_6 during the aluminothermic reaction, at different concentrations.
- Microstructural characterization of AA6063 / ZrB_2 composites, by optical and electron microscopy (SEM, TEM and HRTEM).
- Characterization of composites obtained in-situ by X-ray diffraction (XRD) and energy dispersive spectroscopy (EDS) for different phases formed.
- TEM analysis of the ZrB_2 compound to examine the structure, composition, and properties in detail.
- Vickers microhardness in different areas of composite materials reinforced with ZrB_2 ceramic particles.
- The influence of ZrB_2 on the breaking of composites.
- Analysis of the granulometric distribution as a function of volume for different concentrations of reinforcing particles, resulting from the reactions in the system AA6063 - K_2ZrF_6 - KBF_4 - Na_3AlF_6.
- Vickers microhardness in different areas of functional gradient materials reinforced with ZrB_2 ceramic particles.
- Comparative analysis of expansion coefficients according to the concentrations of reinforcing elements obtained in-situ.
- Comparative analysis of the diffusivity of composite materials AA6063 / ZrB_2, depending on the concentrations of reinforcing elements obtained in-situ.

Future directions of research

1. Analysis of the physical-mechanical behaviour of reinforcing composites with different borons (ZrB_2, TiB_2, VB_2, etc.) and completion of mechanical test tests.
2. Determination and mathematical modelling of other correlations such as tensile strength or modulus of elasticity and some material constants.
3. Obtaining functional gradient materials using AA6063 / ZrB_2 composites as starting materials.

Bibliography

[1] K. U. Kainer, „Metal Matrix Composites Custom-made Materials for Automotive and Aerospace Engineering," în *Basics of Metal Matrix Composites,* Weinheim, WILEY-VCH Verlag GmbH & Co, 2006.

[2] B. Singh, H. Lal, G. Singh și P. Singh, „EFFECT ON PROPERTIES OF ALUMINUM BY ADDING ALUMINA SLAG AS A STRENGTHENER," *International Journal of Mechanical Engineering and Robotics Research,* vol. 2, nr. 3, pp. 96 - 100, 2013.

[3] The Material And Process Requirements In Disc Brake Engineering Essay, „UKEssays," November 2018. [Interactiv]. Available: https://www.ukessays.com/essays/engineering/the-material-and-process-requirements-in-disc-brake-engineering-essay.php.

[4] T. Sornakumar și K. Marimuthu, „Machining studies of die cast aluminum alloy-silicon carbide composites," *International Journal of Minerals, Metallurgy and Materials,* vol. 17, pp. 648-653, 2010.

[5] M. Vinayagam, R. K și M. Ravichandran, „Synthesis, characterization and properties of stir cast AA6351-aluminium nitride (AlN) composites," *Journal of Materials Research,* vol. 31, pp. 1-8, 2016.

[6] X.-H. Chen și H. Yan, „Fabrication of nanosized Al2O3 reinforced aluminum matrix composites by subtype multifrequency ultrasonic vibration," *Journal of Materials Research,* vol. 30, pp. 2197-2209, 2015.

[7] V. Mohanavel, S. S. Kumar, T. Sathish și K. Anand, „Effect of ZrB2 content on mechanical and microstructural characterization of AA6063 aluminum matrix composites," *Materials Today: Proceedings,* vol. 5, nr. 5, pp. 13601-13605, 2018.

[8] B. Cantor, F. Dunne și I. Stone, Metal and Ceramic Matrix Composites, London: Institute of Physics Publishing, 2004.

[9] A. K. Sharma, R. Bhandari, A. Aherwar, R. Rimašauskienė și C. Pinca-Bretotean, „A study of advancement in application opportunities of aluminum metal matrix composites," *Materials Today: Proceedings,* vol. 26, nr. 2, pp. 2419-2424, 2020.

[10] M. Surappa, „Aluminium Matrix Composites: Challenges and Opportunities," *Sadhana,* vol. 28, pp. 319-334, 2003.

[11] W. D. C. Jr. și D. G. Rethwish, „Chapter 16. Composites," în *Materials Science and Engineering An Introduction*, Wiley, 2006, pp. 577-617.

[12] V. K. Balla, K. H. Kate, J. Satyavolu, P. Singh și J. G. D. Tadimeti, „Additive manufacturing of natural fiber reinforced polymer composites: Processing and prospects," *Composites Part B: Engineering,* vol. 174, 2019.

[13] N. Chawla și K. K. Chawla, Metal Matrix Composites, New York: Springer, 2013.

[14] Y. Nishida, Introduction to Metal Matrix Composites. Fabrication and Recycling.

[15] A. M. A. N. Subra Suresh, „Fundamentals of Metal Matrix Composites,” Stoneham, Butterworth-Heinemann, 1993.

[16] M. Zabihi, M. R. Toroghinejad și A. Shafyei, „Application of powder metallurgy and hot rolling processes for manufacturing aluminum/alumina composite strips,” *Materials Science & Engineering A,* nr. 560, pp. 567 - 574, 2013.

[17] A. &. M. D. Bhowmik, „A Comprehensive Study of an Aluminum Alloy AL-5052,” *Advance Physics Letter ,* vol. 3, nr. 1, pp. 20 - 22, 2018.

[18] O. Khayal, „MANUFACTURING AND PROCESSING OF COMPOSITE MATERIALS,” Nile Valley University, 2019.

[19] O. M. E. S. Khayal, „LECTURE NOTES ON MANUFACTURING AND PROCESSING OF COMPOSITE MATERIALS,” Nile Valley University, 2017.

[20] M. Solari și H. Biloni, „Microsegregation in cellular and cellular dendritic growth,” *Journal of Crystal Growth,* vol. 49, nr. 3, pp. 451-457, 1980.

[21] W. Gao, S.-D. Feng, S.-L. Zhang, L. Qi și R.-P. Liu, „Relationship between Voronoi entropy and the viscosity of Zr36Cu64 alloy melt based on molecular dynamics,” *Chinese Physics B,* vol. 24, nr. 12, 2015.

[22] S.-J. Park și M.-K. Seo, „Types of Composites,” în *Interface Science and Composites,* Interface Science and Technology, Elsevier, 2011, pp. 501 - 629.

[23] Y. &. I. Nishida, Norihisa și Y. Kuramasu, „Recycling of aluminum matrix composites,” *Metallurgical and Materials Transactions A,* vol. 30, pp. 839-844, 1999.

[24] N. Chawla și K. K. Chawla, „Interface,” în *Metal Matrix Composites,* New York, NY, Springer New York, 2013, pp. 99 - 119.

[25] J. W. KANG, O. H. KWON și Y. S. YUN, „The investigation of the elastic-plastic behavior using the property gradient of the interfacial region in fiber reinforced MMC,” *International Journal of Modern Physics B,* vol. 20, nr. 15, 2010.

[26] O. M. Alzouma, M.-A. Azman, D.-L. Yung, V. Fridrici și P. Kapsa, „Influence of different reinforcing particles on the scratch resistance and microstructure of different WC–Ni composites,” *Wear,* Vol. %1 din %2352-353, pp. 130-135, 2016.

[27] N. Souissi, S. Souissi, C. Le Niniven, M. Amar, C. Bradai și F. Elhalouani, „Optimization of Squeeze Casting Parameters for 2017 A Wrought Al Alloy Using Taguchi Method,” *Metals - Open Access Metallurgy Journal,* vol. 4, nr. 2, pp. 141 - 154, 2014.

[28] G. U. Umbelino, J. J. F. d. Silva și G. B. P. Ferreira, „Effect of the Additives of Nanosized Nb and Ta Carbides on Microstructure and Properties of Sintered Stainless Steel,” în *Sintering – Methods and Products*, Federal University of Rio Grande do Norte Brazil, 2017.

[29] F. A. Girot, A. P. Majidi și T. W. Chou, „Metal Matrix Composites,” Encyclopedia of Physical Science and Technology (Third Edition), 2003, pp. 485-493.

[30] U.S. Congress, Office of Technology Assessment, Advanced Materials by Design, Washington, DC: U.S: Government Printing Office, June 1988.

[31] G. Manohar, A. Dey, K. M. Pandey și S. R. Maity, „Fabrication of metal matrix composites by powder metallurgy: A review,” *International Conference on Electrical, Electronics, Materials and Applied Science,* vol. 1952, nr. 1, 2018.

[32] Ö. Balcı, D. Ağaoğulları, H. Gökçe, İ. Duman și L. Öveçoğlu, „Influence of TiB2 particle size on the microstructure and properties of Al matrix composites prepared via mechanical alloying and pressureless sintering,” *Journal of Alloys and Compounds,* vol. 586, pp. 78-84, 2014.

[33] Zhu Rui, Yutao Zhao, Songli Zhang, Zhihong Jia, “In situ fabrication and microstructure of ZrB2 particles reinforced aluminum matrix composites”, *Advanced Materials Research*, ISSN 1662-8985, Vols. 476-478, pp. 122-125, Trans Tech Publications, Switzerland, 2012

[34] M. Velashjerdi, H. Sarpoolaky, A. Mirhabibi, „Novel synthesis of ZrB_2 powder by low temperature direct molten salt reaction”, *Ceramics International*, Volume 41, Issue 10, Part A, December 2015, Pages 12554-12559

[35] I. Dinaharan**,** G. Ashok Kumar**,** S.J. Vijay**,** N. Murugan**, „**Development of Al_3Ti and Al_3Zr intermetallic particulate reinforced aluminum alloy AA6061 in situ composites using friction stir processing”**,** *Materials and Design*, Volume 63, November 2014, Pages 213-222

[36] Xizhou Kai, Yutao Zhao, Andong Wang, Chunmei Wang, Zemin Mao, „Hot deformation behavior of in situ nano ZrB_2 reinforced 2024Al matrix composite”, *Composites Science and Technology* 116, (2015), 1 - 8

[37] M. Velashjerdi, H. Sarploolaky, A. Mirhabibi, „The effect of different molten salt composition on morphology and purity of the ZrB_2 powder obtained via direct molten salt reaction method”, *Journal of Advanced Materials and Processing,* Vol. 3, nr. 3, 2015, pp. 25-34

[38] Gaurav Gautam, Narendra Kumar, Anita Mohan, Sunil Mohan, R.K. Gautam, „Synthesis and tribological properties of AA5052 base in situ composites”, *Proceeding of Malaysian International Tribology Conference,* 2015, November, pp. 117-119

[39] Narendra Kumar, Rakesh Kumar Gautam, Sunil Mohan, „In-situ development of ZrB_2 particles and their effect on microstructure and mechanical properties of AA5052 metal-matrix composites”, *Materials and Design*, Volume 80, 5 September 2015, Pages 129-136

[40] Kangle Tian, Yutao Zhao, Lei Jiao, Songli Zhang, Zhenya Zhang, Xiuchuan Wu, „Effects of in situ generated ZrB_2 nano-particles on microstructure and tensile properties of 2024Al matrix composites”, *Journal of Alloys and Compounds,* Volume 594, 5 May 2014, Pages 1-6

[41] N. Mathan Kumar, S. Senthil Kumaran, L. A. Kumaraswamidhas, „An investigation of mechanical properties and corrosion resistance of Al2618 alloy reinforced with Si_3N_4, AlN and ZrB_2 composites”, *Journal of Alloys and Compounds*, Volume 652, 15 December 2015, Pages 244-249

[42] V. Mohanavel, M. Naveen Kumar, K. Mageshkumar, C. Jayasekar, N. Dineshbabu, S. Udishkumar, „Mechanical behavior of in situ ZrB_2/AA2014 composite produced by the exothermic salt-metal reaction technique", *Materials Today Proceedings*, Volume 4, Issue 2, Part A, 2017, Pages 3215-3221

[43] Song-Li Zhang, Yu-Tao Zhao, Gang Chen, Xiao-Nong Cheng, Xiao-Yang Huo, „Fabrication and dry sliding wear behavior of in situ Al–K_2ZrF_6–KBF_4 composites reinforced by Al_3Zr and ZrB_2 particles", *Journal of Alloys and Compounds*, Volume 450, Issues 1–2, 14 February 2008, Pages 185-192

[44] G. Naveen Kumar, R. Narayanasamy, S. Natarajan, S. P. Kumaresh Babu, K. Sivaprasad, S. Sivasankaran, „Dry sliding wear behaviour of AA 6351-ZrB_2 in situ composite at room temperature", *Materials and Design*, Volume 31, Issue 3, March 2010, Pages 1526-1532

[45] Yutao Zhao, Songli Zhang, Gang Chen, Xiaonong Cheng, „Effects of molten temperature on the morphologies of in situ Al_3Zr and ZrB_2 particles and wear properties of (Al_3Zr + ZrB_2)/Al composites", *Materials Science and Engineering*: A, Volume 457, Issues 1–2, 25 May 2007, Pages 156-161

[46] Songli Zhang, Yutao Zhao, Gang Chen, Xiaonong Cheng, „Microstructures and dry sliding wear properties of in situ (Al_3Zr + ZrB_2)/Al composites", *Journal of Materials Processing Technology*, Volume 184, Issues 1–3, 12 April 2007, Pages 201-208

[47] J. David Raja Selvam, I. Dinaharan, „In situ formation of ZrB_2 particulates and their influence on microstructure and tensile behavior of AA7075 aluminum matrix composites", *Engineering Science and Technology*, an International Journal, Volume 20, Issue 1, February 2017, Pages 187-196

[48] Gaurav Gautam, Anita Mohan, „Effect of ZrB_2 particles on the microstructure and mechanical properties of hybrid (ZrB_2 + Al_3Zr)/AA5052 *in situ* composites", *Journal of Alloys and Compounds*, Volume 649, 15 November 2015, Pages 174-183

[49] R. Vasanth Kumar, R. Keshavamurthy, Chandra S. Perugu, Praveennath G. Koppad, Mohammad Alipour, „Influence of hot rolling on microstructure and mechanical behaviour of Al6061-ZrB_2 in-situ metal matrix composites", *Materials Science and Engineering: A*, Volume 738, 19 December 2018, Pages 344-352

[50] J. Jenix Rino, S. Balasivanandha Prabu, R. Paskaramoorthy, „Comparison of thermal and mechanical properties of Al-5wt.%TiB_2 and Al-5wt.%ZrB_2 composites processed through salt-melt reaction route", *Materials Today: Proceedings*, Volume 4, Issue 8, 2017, Pages 8739-8750

[51] J. B. Fogagnolo, M. H. Robert, E. M. Ruiz-Navas, J. M. Torralba, „6061 Al reinforced with zirconium diboride particles processed by conventional powder metallurgy and mechanical alloying", *Journal of Materials Science* 39 (2004) 127 – 132

[52] I. Dinaharan, N. Murugan, Siva Parameswaran, „Influence of in situ formed ZrB_2 particles on microstructure and mechanical properties of AA6061 metal matrix composites", *Materials Science and Engineering: A*, Volume 528, Issue 18, 15 July 2011, Pages 5733-5740

[53] W. G. Fahrenholtz, G. E. Hilmas, I. G. Talmy și J. A. Zaykoski, „Refractory Diborides of Zirconium and Hafnium", *J. Am. Ceram. Soc*, Vol. 90, 2007, pp. 1347–1364.

[54] B. Post, F. W. Glaser și D. Moskowitz, „Structural Transition Metal Diborides”, *Acta. Metal.*, Vol. 2, 1954, pp. 20-25.

[55] J. K. Sonber, A. K. Suri, „Synthesis and Consolidation of Zirconium Diboride : review”, *Adv. App. Ceram*, Vol. 110, 2011, pp. 321–334.

[56] M. Jalaly, M. Tamizifar, M. S. Bafghi și F. J. Gotor, „Mechanochemical synthesis of ZrB2-SiC- ZrC nanocomposite powder by metallothermic reduction of zircon”, *J. Alloys Compd.*, Vol. 581, 2013, pp. 782–787.

[57] S. Motojima, K. Funahashi și K. Kurosawa, „ZrB2 coated on copper plate by chemical vapour deposition and its corrosion and oxidation stabilities”, *Thin Solid Films*, Vol. 189, 1990, pp. 73–79.

[58] B. Yang, J. Li, B. Zhao, Y. Hu, T. Wang, D. Sun, R. Li, S. Yin, Z. Feng, Q. Tang și T. Sato, „Synthesis of hexagonal-prism-like ZrB2 by a sol – gel route”, *Powder Technol.*, Vol. 256, 2014, pp. 522–528.

[59] S. E. Kravchenko, V. I. Torbov și S. P. Shilkin, „Nanosized zirconium diboride: Synthesis and properties”, *Russ. J. Inorg. Chem.*, Vol. 56, 2011. pp. 506–509.

[60] T. Y. Kosolapova, T. I. Serebryakova, I. Popova și V. I. Babich, „Impurities in ZrB2 Prepared by Different Methods”, *J. Less. Com. Metal*, Vol. 7, 1979, pp. 303–307.

[61] P. Afanasiev, C. Geantet și C. Geantet, „Synthesis of Solid Materials in Molten Nitrates”, *Cord. Chem. Rev*, Vol. 180, 1998, pp. 1725– 1752.

[62] B. Roy, S. P. Ahrenkiel și P. A. Fuierer, „Controlling the Size and Morphology of TiO2 Powder by Molten and Solid Salt Synthesis”, *J.Am. Ceram. Soc.*, Vol. 91, 2008, pp. 2455–2463.

[63] S. Zhang, M. Khangkhamano, H. Zhang și H. A. Yeprem, „Novel Synthesis of ZrB2 Powder via Molten – Salt - Mediated Magnesiothermic Reduction”, *J. Am. Ceram. Soc.*, Vol. 97, 2014, pp. 1686–1688.

[64] M. Velashjerdi, H. Sarpoolaky și A. R. Mirhabibi, Novel synthesis of ZrB2 powder by low temperature direct molten salt reaction, *Ceram. Iner*, Accepted manuscript.

[65] Y. Zhao, S. Zhang, G. Chen, and X. Cheng, „Effects of Molten Temperature on the Morphologies of in Situ Al3Zr and ZrB2 Particles and Wear Properties of (Al3Zr + Zrb2)/Al Composites”, *Mater. Sci. Eng. A*, Vol. 457, 2007, pp. 156–161.

[66] Degang Zhao, Xiangfa Liu, Yuxian Liu, Xiufang Bian, Journal of Materials Science 40 (2005) 4365-4368.

[67] I. Barin and O. Knache, “Thermochemical Properties of Inorganic Substances”, Springer, Berlin, New York, 1973, p.792.

[68] Songli Zhang, Yutao Zhao, Gang Chen, Xiaonong Cheng, Journal of Materials Processing Technology 184 (2007) 201-208.

[69] Xunyin Zhang, Guirong Li, Tingwang Zhang, Lei Cao, Hongming Wang, Jun-Jie Wang, Kai-Xuan Gu, Hong Zhang, Xiao-Jing Xu, Applied Mechanics and Materials Vols. 217-219 (2012) pp 114-118.

[70] Bekir Sadik Unlum and Enver Atik, Mat. Design, vol. 30, (2009), p. 1381.

[71] Zhu Rui, Yu Tao Zhao, Song Li Zhang, Zhi Hong Jia, Advanced Materials Research (Volumes 476-478) 2012, p. 122-125, Trans. Tech. Publications, Switzerland.

[72] Kangle Tian, Yutao Zhao, Lei Jiao, Songli Zhang, Zhenya Zhang, Xiuchuan Wu, Journal of Alloys and Compounds 594 (2014) 1-6.

[73] Xizhou Kai, Yutao Zhao, Andong Wang, Chunmei Wang, Zemin Mao, Composites Science and Technology 116 (2015) 1-8.

[74] Narendra Kumar, Rakesh Kumar Gautam, Sunil Mohan, Materials and Design 80 (2015) 129-136.

[75] Gaurav Gautam, Anita Mohan, Journal of Alloys and Compounds 649 (2015) 174-183.

[76] V.M. Sreekumar and D.G. Eskin, JOM, Vol. 68, No. 12, 2016.

[77] J. David Raja Selvam, I. Dinaharan, Engineering Science and Technology 20 (2017) 187-196.

[78] Rui Yang, Zhenya Zhang, Yutao Zhao, Gang Chen, Manping Liu, Lei Jiao, Ling Chen, Materials Characterization 112 (2016) 51-59.

[79] V. Mohanavela, M. Naveen Kumara, K. Mageshkumara, C. Jayasekara, N. Dineshbabua, S. Udishkumar, Materials Today: Proceedings 4 (2017) 3215-3221.

[80] Manea, Ciprian Alexandru; Csaki, Ioana; Geambazu, Laura Elena; Miculescu, Florin; Petrescu, Mircea Ionut; Fanicchia, Francesco; Sohaciu, Mirela; Roșu, Lucian: HfNbTaTiZr HIGH ENTROPY ALLOY PROCESSED BY MECHANICAL ALLOYING, U.P.B. Sci. Bull., Series B, Vol.81, Iss. 3, Pag. 201-208, 2020, ISI, WOS:000487215400020.

[81] Buțu Mihai, Moldovan Petru, Roșu Lucian, Stăncel Constantin, Ogica Cătălin, Buțu Larisa, Marinescu Marilena, RESEARCH STUDIES ON OBTAINING METASTABLE INTERMETALLIC STRUCTURES IN 6xxx/BORIDES COMPOSITES, U.P.B SCI. BULL. SERIES B-CHEMISTRY AND MATERIALS SCIENCE, VOL 82, nr. 2, 2020, pag. 185-198, ISSN 1454-2331, WOS:000550842800017

[82] R. D. Cowan, "Pulse Method of Measuring Thermal Diffusivity at High Temperatures", Journal of Applied Physics, 34 (4): 926, (1963)

[83] J. A. Cape, G. W. Lehman, "Temperature and Finite-Pulse-Time Effects in the Flash Method for Measuring Thermal Diffusivity", Journal of Applied Physics, 34 (7): 1909, (1963)

[84] U. S. Patent 7038209, J. Blumm, J. Opfermann, "Improvement of the mathematical modeling of flash measurements", High Temperatures – High Pressures, 34 (5): 515, (2002)